Quantum optics of localized light in a photonic band gap

Sajeev John and Jian Wang
Department of Physics, University of Toronto, 60 St. George Street, Toronto, Ontario, Canada M5S 1A7
(Received 21 September 1990)

We describe the quantum electrodynamics of photons interacting with hydrogenic atoms and molecules in a class of strongly scattering dielectric materials. These dielectrics consist of an ordered or nearly ordered array of spherical scatterers with real positive refractive index and exhibit a complete photonic band gap or pseudogap for all directions of electromagnetic propagation. For hydrogenic atoms with a transition frequency in the forbidden optical gap, we demonstrate both the existence and stability of a photon-atom bound state. For a band gap to center frequency ratio $\Delta\omega/\omega_0 \sim 5\%$, the photon localization length $\xi_{\rm loc} \geq 10L$, where L is the lattice constant of dielectric array. This strong self-dressing of the atom by its own localized radiation field leads to anomalous Lamb shifts and a splitting of the excited atomic level into a doublet when the transition frequency lies near a photonic band edge. We estimate the magnitude of this splitting to be 10^{-6} at the vacuum transition energies. The stability of this photon-bound state with respect to electromagnetic as well as vibrational decay mechanisms is examined. For an isolated molecule embedded in the solid fraction of the dielectric structure, the dominant mechanism for absorption and spontaneous emission is via optically driven electron-phonon interactions and the resulting phonon-absorption and -emission sidebands. Raman or Brillouin scattering of a localized photon into a propagating mode, or vice versa, directly by photon-phonon interaction is forbidden. For atoms not in contact with the solid fraction of the dielectric host, the electromagnetic two-photon spontaneous emission rate is on the scale of several days. For two identical atoms separated by a distance R within the photonic band gap, energy transfer from an excited atom to an unexcited atom occurs by a phase-shifted resonance dipole-dipole interaction which vanishes exponentially for $R > \xi_{\rm loc}$. This leads to the formation of a narrow photonic impurity band within the gap when a finite density of atoms is present. This impurity band exhibits a different kind of nonlinear optical properties. When two neighboring atoms are both excited, single-photon spontaneous emission at $\sim 2\hbar\omega_0$ occurs by a third-order electromagnetic process with rate $\Gamma \sim \alpha^3\omega_0(a_0/R)^8$, where a_0 is the atomic Bohr radius and α is the fine-structure constant.

I. INTRODUCTION

Recent experimental investigations[1-4] of electromagnetic propagation in strongly scattering dielectric materials have demonstrated the observability of the strong localization of photons[5-7] in analogy with the Anderson localization of electrons in disordered solids.[8] These dielectric materials constitute the optical analog of electronic semiconductors. The spherical dielectric scatterers have a size comparable to the wavelength of light, and the associated Mie resonances play an analogous role to the electronic energy levels in an atom. For a large collection of spheres, coherent multiple scattering gives rise to the phenomenon of weak localization.[9-12] When strong spatial correlations exist between individual scatterers, the phase space available to the multiply scattered wave can be severely reduced. For electrons in a periodic solid, this gives rise to electronic band structure. Likewise for optical waves, correlations among optically connected spheres lead to a suppression of the photon density of states over a narrow frequency range. This suppression is most dramatic at sphere densities for which there is a synergetic interplay between single-scattering Mie resonances and macroscopic Bragg scattering. The resulting photonic band gap has been experimentally observed by Yablonovitch and Gmitter[3] in the microwave-frequency regime. For a lossless, periodic dielectric material with refractive index 3.5 containing a fcc lattice of spherical air cavities, an almost complete photonic band gap has been observed when the volume-filling fraction of the high-dielectric material is approximately 0.15. For a frequency range spanning about 6% of the gap center frequency, propagating electromagnetic modes are absent in all but a few directions.

Some very recent studies have suggested that the use of nonspherical scatterers or lattices with a nontrivial basis might be even more effective in producing a complete photonic band gap rather than a pseudogap.[12] Band-structure calculations have shown that a complete gap may be produced with refractive index $n \geq 2.0$ using a diamond lattice structure. Furthermore, Yablonovitch and his collaborators have found a complete microwave band gap of width about 20% of the gap-center frequency using cylindrical rather than spherical dielectric microstructures.[12]

The existence of such a photonic band gap in a periodic dielectric or the related strong localization pseudogap in the corresponding disordered dielectric have important consequences both at the classical and quantum-mechanical levels. In this paper we present a detailed investigation of the quantum-electrodynamic interaction of localized light with atoms and molecules placed within the dielectric medium. The photon-atom bound state predicted previously[13] is examined by means of two

separate model Hamiltonians for electromagnetic band structure. In the first model, the band gap is chosen to be isotropic in the photon wave-vector space. Although this model gives a good qualitative picture, it artificially overestimated the available phase space for optical propagation near a band edge. The near-band-edge behavior is studied by means of a separate anisotropic model based on the "nearly-free-photon approximation" in analogy to the nearly-free-electron approximation for electronic band structure in a weak periodic potential.[7] Near the band edge, an "effective-mass approximation" to the vector band structure yields a quantum electromagnetic splitting of the hydrogenic $2p_{1/2}$ level into a doublet. The predicted splitting is of order $10^{-6}\hbar\omega_0$, where $\hbar\omega_0$ is the vacuum $2p \rightarrow 1s$ transition energy. This is larger than the normal vacuum Lamb shift of the $2p$ level relative to the $2s$ level and arises from the resonant interaction of photons of vanishing group velocity with the atom. It is analogous to the well-known Mollow resonances[14] observed when an atom is irradiated by an intense laser field. Unlike the externally dressed atomic states associated with Mollow level splittings, the atom near a photonic band edge is dressed by its own localized radiation field. The localized electromagnetic mode is the photonic analog of a localized electron-impurity level in the gap of a traditional semiconductor. In a three-dimensional semiconductor, gap states are associated with strong scattering by a defect or impurity. In the optical case, this strong coupling of the photon to the impurity atom is guaranteed by the absence of single-photon spontaneous emission. Despite the smallness of the fine-structure constant, the effective atomic polarizability near resonance, which is normally limited by the natural linewidth, is now arbitrarily large.

Since propagating electromagnetic modes are absent in the gap region, any mechanism for coupling energy into or out of the localized optical mode will involve some nonlinear process. For an impurity atom which is embedded in a solid dielectric host, the vibrational modes of the host will provide a possible relaxation mechanism for the photon-bound state. It is noteworthy that the traditional photon-phonon interactions normally responsible for spontaneous Brillouin and Raman scattering in the bulk are ineffective in inelastically scattering a localized photon within the gap to an extended electromagnetic mode outside of the gap. The matrix element for such a process involves the overlap integral of the localized photon state vector with that of an extended state, and this quantity vanishes identically in the thermodynamic (large sample volume) limit. On the other hand, vibrational motion of host atoms in the vicinity of the impurity molecule can adiabatically alter the electronic spectrum of the impurity. Whereas the optical field drives the electron, the electron can in turn drive phonon-emission and -absorption sidebands which accompany the electronic transition. These vibrational modes carry away or provide the necessary energy to couple the localized photon to a propagating mode outside of the gap. These vibrational relaxation mechanisms will invariably supersede the electromagnetic relaxation via two-photon spontaneous emission, which we estimate occurs on the time scale of several days.

When a collection of identical impurity atoms is placed within the photonic band gap, we anticipate the occurrence of a variety of electromagnetic phenomena arising from cooperative activity of the many-body system. For a trivial band gap to center frequency ratio $\Delta\omega/\omega_0 \sim 5\%$, the localization or tunneling distance of the photon from the impurity atom $\xi_{\rm loc} \geq 10L$, where the lattice constant of the periodic dielectric, $L \sim \lambda$, the photon wavelength. It follows that for a pair of atoms separated by a distance $R < \xi_{\rm loc}$, there will be significant electromagnetic coupling. In particular, if one atom is excited and the other in its ground state, the localized photon can hop to the unexcited atom by the resonance dipole-dipole interaction (RDDI). An estimate of this hopping matrix element is given by $M \sim (\mu^2/a_0^3)(a_0/R)^3$, where the atomic dipole moment $\mu \sim ea_0$. Here a_0 is the atomic Bohr radius. However, we anticipate that $\mu^2/a_0^3 \sim \hbar\omega_0$ so that for a typical gas density for impurity atoms, the interaction M is at least 3 orders of magnitude less than $\hbar\omega_0$. For a large collection of impurity atoms spaced by $R \sim 10$ Å, a narrow photonic impurity band for electromagnetic hopping conduction will arise within the larger photonic band gap. Recently, Kurizki[15] has pointed out that the RDDI matrix element may undergo a $\pi/2$ phase shift relative to its vacuum value in addition to exponentially decay for $R > \xi_{\rm loc}$. Such a phase shift can alter the nature of molecular interaction and reaction chemistry within a dielectric exhibiting a photonic band gap. This result was obtained within an effective-mass approximation to the photonic band structure. This approximation is valid only on length scales $R \gg \lambda$, the photon wavelength. At short distance $R \ll \lambda$, we find that $M \sim \hbar\omega_0(a_0/R)^3$, although the constant of proportionality may vary depending on position of the atomic transition relative to the photonic band edges.

The photonic impurity band described above will exhibit nonlinear optical properties by virtue of its strong coupling to the impurity atom's electronic degrees of freedom. For example, when two neighboring atoms separated by a distance R are both excited, there is an amplitude for second-harmonic generation of a single photon of energy $\sim 2\hbar\omega_0$. This gives rise to a weak spontaneous emission out of the photonic band gap with a rate given approximately by $\Gamma \sim \alpha^3\omega_0(a_0/R)^8$, where α is the fine-structure constant. This arises from virtual two-photon excitation of a single atom and its subsequent decay. These various electromagnetic and vibrational interactions constitute the basic building blocks of cooperative behavior such as superradiance and lasing action of this novel quantum many-body system. We now proceed to give a detailed derivation of these effects.

Briefly, this paper is organized as follows: In Sec. II we introduce the model Hamiltonian for electromagnetic band structure and describe the formation of a single photon-atom bound state. In Sec. III we derive the properties of two-photon spontaneous emission from a single atom. In Sec. IV we derive the nature of hopping conductivity of photons within the gap arising from resonance dipole-dipole interaction between atoms. In Sec. V we calculate the rate of two-photon pair annihilation and

the resulting second-harmonic generation for a two neighboring excited atoms. In Sec. VI we discuss qualitatively possible relaxation processes that are mediated by the vibrational degrees of freedom of the dielectric host in which the impurity atoms is embedded. Finally, in Sec. VII we summarize our results.

II. PHOTON-ATOM BOUND STATE

In order to describe quantum electrodynamics within a strong-localization photonic band gap, it is necessary to characterize the underlying electromagnetic band structure. Theoretical work was initiated by John and Rangarajan[16] using the KKR method to compute the band structure for a classical scalar wave scattering from a fcc lattice of dielectric spheres in a uniform background. It was found that the lowest-energy band gap was associated with lowest scalar Mie resonance of a single sphere. For a refractive index ratio of 2.8:1, the largest band gap occurs at a volume-filling fraction of spheres in the 10–15 % range. This has subsequently been reanalyzed by Economou and Zdetsis[17] using the APW method, Satpathy, Zhang, and Salehpour[18] using a plane-wave expansion and Leung and Liu[19] using both plane-wave and higher-order KKR. It is now generally agreed that for scalar waves, the minimum required refractive-index ratio for the creation of a total gap in the photon density of states is about 1.5:1 at a volume-filling fraction of 0.1–0.4. For physical electromagnetic waves, there are no quantitative band structures published, but it is certain that higher refractive-index ratio will be needed because of the extra polarization degree of freedom, and it is likely that higher volume-filling fractions will be required because of the absence of the lowest-order ($l=0$) Mie resonance in this case.

For the purpose of discussion, we introduce a simple isotropic model Hamiltonian (model I) for electromagnetic waves in a three-dimensional periodic dielectric. The photon dispersion relation $\omega_{\mathbf{k}}$ is chosen to be isotropic and to satisfy the transcendental equation

$$4n\cos(kL)=(1+n)^2\cos\left[(2na+b)\frac{\omega_{\mathbf{k}}}{c}\right] -(1-n)^2\cos\left[(2na-b)\frac{\omega_{\mathbf{k}}}{c}\right] . \tag{2.1}$$

The photon energy $\hbar\omega_k$ obtained by solving this equation is in fact the exact solution of the scalar wave equation in one dimension (see Appendix):

$$-\nabla^2\phi-\frac{\omega^2}{c^2}\epsilon(x)\phi=\frac{\omega^2}{c^2}\phi , \tag{2.2a}$$

with dielectric constant

$$\epsilon(x)=\sum_{m=-\infty}^{\infty}u(x-mL) , \tag{2.2b}$$

where

$$u(x)=\begin{cases}n^2-1, & |x|<a ,\\ 0, & \text{otherwise} .\end{cases}$$

Here n is the refractive index of the scatterer, a is its radius, and $2a+b=L$ is the lattice constant. To complete the definition of the electromagnetic properties of the dielectric, we assume that the normal modes are plane waves of the form $\mathbf{e}_{\lambda\mathbf{k}}e^{i\mathbf{k}\cdot\mathbf{r}}/\sqrt{\Omega}$, where Ω is the volume of the dielectric sample and the polarization vectors satisfy the transversality condition $\sum_{\lambda=1}^{2}e^{i}_{\lambda\mathbf{k}}e^{j*}_{\lambda\mathbf{k}}=(\delta_{ij}-\hat{k}_i\hat{k}_j)$. By symmetrizing $\omega_{\mathbf{k}}$ given in Eq. (2.1) to all directions in $\mathbf{k}$ space, we produce photonic band gaps at the spheres $|\mathbf{k}|=m\pi/L$, with $m=1,2,3,\ldots$. This procedure artificially increases the true phase space available for photon propagation near a band edge, and the corresponding density of states becomes singular. In a real three-dimensional (3D) crystal, the gap is highly anisotropic. We defer a discussion of quantitative corrections to our model near a band edge since it leads to qualitatively correct physics. The dispersion relation [Eq. (2.1)] exhibits many features of the observed as well as computed band structure in 3D. For example, an approximate value of the optimum high refractive-index volume fraction for the creation of a large band gap follows from a simple argument. The dielectric "potential" $u(x)$ has the analog of a Mie resonance when precisely a quarter-wavelength $(2\pi c/\omega n)/4$ fits into the diameter $2a$. A "Mie" resonance here is defined as a minimum in the transmission coefficient. On the other hand, a Bragg scattering resonance occurs when $\omega/c=\pi/L$. The condition that both the Bragg and Mie resonances occur at the *same* frequency is the condition that the volume-filling fraction $f\equiv 2a/L=1/2n$. An optimum volume-filling fraction of this nature has been observed experimentally[3] and in scalar wave band structures.[16]

For the special case $2na=b$, Eq. (2.1) can be solved analytically to give

$$\omega_k=\frac{c}{4na}\arccos\left[\frac{4n\cos(kL)+(1-n)^2}{(1+n)^2}\right] , \tag{2.1'}$$

where ω, as a function of the complex variable k, has branch-cut singularities for $k=m\pi/L$ with the gap vanishing for even values of m. The spectrum for real k and the corresponding density of states are depicted in Fig. 1(a). In the complex k plane, ω_k has branch-cut singularities as shown in Fig. 1(b).

We consider the quantum electrodynamics of a hydrogenic atom which is minimally coupled to the radiation field defined by Eq. (2.1). The Hamiltonian for the coupled system may be written as

$$H=H_{\text{atom}}+H_{\text{rad}}+H_{\text{int}}+H_{\text{ct}} , \tag{2.3}$$

where

$$H_{\text{atom}}=\frac{\mathbf{p}^2}{2m}+V(\mathbf{r}) ,$$

$$H_{\text{rad}}=\sum_{\mathbf{k}\lambda}\hbar\omega_{\mathbf{k}}a^{\dagger}_{\mathbf{k}\lambda}a_{\mathbf{k}\lambda} ,$$

$$H_{\text{int}}=\frac{e}{mc}\mathbf{p}\cdot\mathbf{A}(\mathbf{r})+\frac{e^2}{2mc^2}\mathbf{A}^2 ,$$

and $H_{\text{ct}}=(\delta m/m)p^2/2m$ is a mass-renormalization counterterm for an electron of observable mass m. We assume bare atomic eigenstates with energies E_n, for $n=0,1,2,\ldots$. In the electric dipole approximation, we

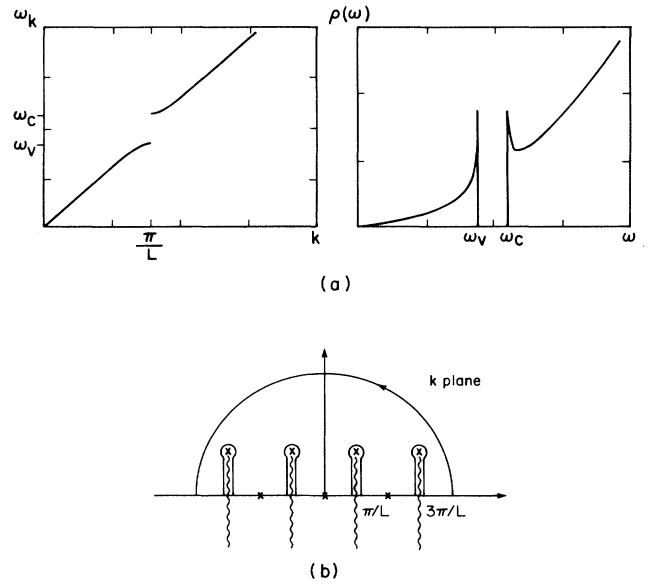

FIG. 1. (a) Dispersion relation and the corresponding density of states for the isotropic model. (b) Branch cut of ω_k of Eq. (2.1a) in the complex k plane.

neglect the electron coordinate $\mathbf{r}$ dependence of the vector potential in the evaluation of any matrix elements.

An approximate eigenstate of the Hamiltonian [Eq. (2.3)] in the one-photon sector of the entire Hilbert space may be determined by introducing a trial wave function

$$|\psi\rangle=\sum_{n=1}^{\infty}\phi_n|n\rangle+\sum_{n=0}^{\infty}\sum_{\mathbf{k}\lambda}\psi_{\mathbf{k}\lambda}^{(n)}|\mathbf{k}\lambda;n\rangle\ , \tag{2.4}$$

where $|\mathbf{k}\lambda;n\rangle$ denotes a state in which there is a single photon in model $(\mathbf{k},\lambda)$ and the atom is in its nth excited state. In the state $|n\rangle$ the atom has been excited and the photon absorbed. For a single photon of energy $\hbar\omega_k\simeq E_1-E_0$, the dominant coefficients in the wave-function expansion are ϕ_1 and $\psi_{\mathbf{k}\lambda}^{(0)}$. All other coefficients are higher order in an expansion of the fine-structure constant $\alpha\equiv e^2/(4\pi\epsilon_0\hbar c)$. If we consider electron-mass renormalization to order α, the approximate Schrödinger equation $H|\psi\rangle=E|\psi\rangle$ can be expressed as a set of coupled equations for the expansion coefficients:

$$(E-E_n)\phi_n=\frac{e}{m}\sum_{\substack{\mathbf{k}\lambda\\ l}}\left[\frac{\hbar}{2\epsilon_0\omega_{\mathbf{k}}}\right]^{1/2}\frac{e^{i\mathbf{k}\cdot\mathbf{r}}}{\sqrt{\Omega}}\mathbf{e}_{\lambda\mathbf{k}}\cdot\mathbf{p}_{nl}\psi_{\mathbf{k}\lambda}^{(l)}+\frac{\delta m}{m}K_{n1}\phi_1 \tag{2.5a}$$

and

$$(E-E_n-\hbar\omega_{\mathbf{k}})\psi_{\mathbf{k}\lambda}^{(n)}=\frac{e}{m}\sum_{l=0}^{\infty}\left[\frac{\hbar}{2\epsilon_0\omega_{\mathbf{k}}}\right]^{1/2}\frac{e^{-i\mathbf{k}\cdot\mathbf{r}}}{\sqrt{\Omega}}\mathbf{e}_{\lambda k}^{*}\cdot\mathbf{p}_{nl}\phi_l\ . \tag{2.5b}$$

Here $K_{n1}\equiv\langle n|(p^2/2m)|1\rangle$ and $\mathbf{p}_{nl}\equiv\langle n|\mathbf{p}|l\rangle$. Also, we have chosen units in which the speed of light in vacuum $c=1$.

The amplitude $\psi_{\mathbf{k}\lambda}^{(n)}$ may be eliminated by substituting (2.5b) into (2.5a). If we then neglect the amplitudes ϕ_n except the dominant one ϕ_1, we obtain an approximate eigenvalue equation for the energy E of the coupled atom-radiation field:

$$E-E_1\simeq\frac{e^2}{6\pi^2\epsilon_0\hbar m^2}\sum_{n=0}^{\infty}|\mathbf{p}_{1n}|^2(E-E_n)g(E-E_n)\ , \tag{2.6a}$$

where

$$g(E)\equiv\int_0^{\Lambda}dk\frac{k^2}{\omega_k^2(E/h-\omega_k)},\quad \Lambda\equiv\frac{mc}{\hbar}\ . \tag{2.6b}$$

Here we have used the mass-renormalization counterterm to cancel the linearly divergent part of the sum over $\mathbf{k}$. Following Bethe,[20] we introduce a cutoff Λ in the photon wave vector since photons of energy higher than the electron rest mass mc^2 probe the relativistic structure of the electron wave packet.[21] The standard nonrelativistic perturbation theory result[20] for the Lamb shift of the level E_1 follows by setting $E=E_1$ in the right-hand side of Eq. (2.6) and solving for E. If the atomic level E_1 lies in the allowed spectrum $\hbar\omega_{\mathbf{k}}$, the integral over k is interpreted as a principal value. More generally, we may consider exact solutions of Eq. (2.6) for the complex variable E. The function $g(E)$ has branch-cut singularities at energies in the allowed electromagnetic spectrum and care must be taken in defining the multivalued function. In particular, the phenomenon of resonance fluorescence appears as a solution to Eq. (2.6) in the lower half of the complex E plane on the second Riemann sheet. Analytic continuation to this second sheet is obtained by evaluating $\lim_{\epsilon\to 0}g(E+i\epsilon)$ for real E and letting E be a general complex number in the resulting expression. For real E in the vicinity of E_1, this means

$$E-E_1=\frac{e^2}{6\pi^2\epsilon_0\hbar m^2}\left[\sum_{n=0}^{\infty}|\mathbf{p}_{1n}|^2(E-E_n)\mathrm{P}[g(E-E_n)]-i\pi|\mathbf{p}_{10}|^2E\int_0^{\Lambda}dk\frac{k^2}{\omega_k^2}\delta\left[\frac{E}{\hbar}-\omega_k\right]\right]. \tag{2.7}$$

Here we have chosen $E_0=0$ and P denotes principal value.

This eigenvalue equation always has a solution for some real value of E which lies in the photonic band gap as depicted graphically in Fig. 2 provided E_1 is in or near the gap. Here we have chosen the refractive index $n=1.082$, yielding a gap center frequency $\omega_0=(\pi/L)[(1+n)/2n]c$ and relative gap width $\Delta\omega/\omega_0=0.05$. This small value of the refractive-index contrast is an artifact of the isotropic model. A more realistic model which incorporates the anisotropy of the Brillouin zone would require a much larger value of n for the creation of a total gap. The numerical solution of Eq. (2.7) was facilitated by use of the known dipole matrix

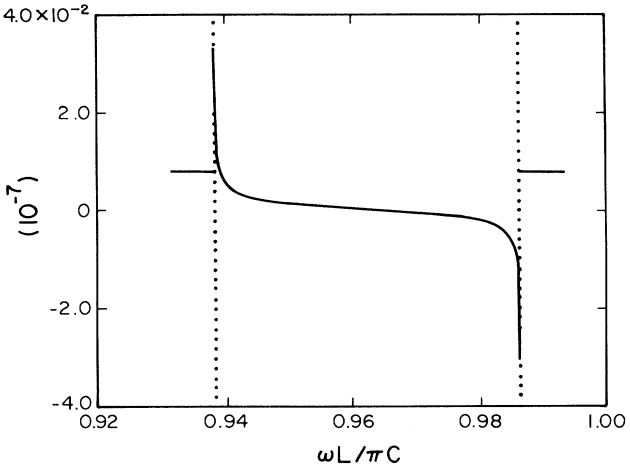

FIG. 2. We plot the right-hand side of Eq. (2.7) measured in units of $\hbar\omega_0$ as a function of $\omega L/\pi c$, for $\omega \equiv E/\hbar$ near or within the band gap. The dotted lines mark the lower and upper band edges.

elements $\mathbf{p}_{1n}$ for discrete and continuum states of hydrogen.[22] This solution corresponds to a bound state of the photon to the atom and occurs despite the weakness of the minimal-coupling interaction [Eq. (2.3)] because of the resonant interaction between the radiation field and the atom. In Fig. 3 we plot the Lamb shift and the tunneling distance (localization length) of the bound photon as E_1 is varied from being just below the gap to just above the gap. This is done for E_1 corresponding to the $2p_{1/2}$ state as well as the $2s_{1/2}$ state of hydrogen.

Near the upper and lower band edges, an additional strong-coupling effect arises from the resonant interaction of the atom with photons whose group velocity $d\omega_k/dk$ vanishes. It follows that when E_1 is close to a band edge, and provided that $|\mathbf{p}_{10}|^2$ is nonzero, the

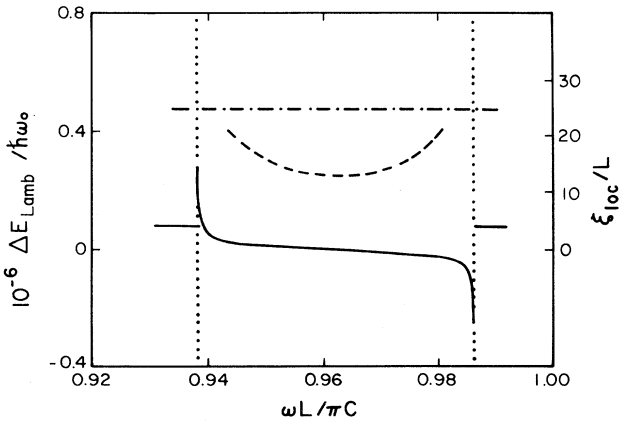

FIG. 3. Lamb shift for the $2p_{1/2}$ state (solid line) and $2S_{1/2}$ state (dot-dashed) measured in units of ω_0 within the band gap. Here $\omega \equiv E_1/\hbar$. At the band edge, the Lamb shift for the $2p_{1/2}$ state reaches a finite value. Here we also plot localization length ξ/L within the band gap (dashed line).

quantum-electrodynamic interaction is sufficiently strong to split the atomic level into a doublet. This is apparent from the graph of Fig. 2 since the function $E-E_1$ intersects the real part of the photon propagator at two energies.

It is straightforward to verify from Eq. (2.7) that for the vacuum case $\omega_k = ck$, the single complex solution on the second Riemann sheet (negative imaginary part for E) describes the correct single-photon-spontaneous-emission rate $1/\tau_1$ from the Lamb-shifted level E. In particular, $1/\tau_1 = 2|\mathrm{Im}E|$. Near a band edge of the dielectric material, it is instructive to analytically estimate the corresponding complex solutions. We consider an effective-mass approximation to the dispersion relation (2.1) for $k \simeq k_0 \equiv \pi/L$. Near the upper band edge ω_c, $\omega_k \simeq \omega_c + A(k-k_0)^2$. For the special case $b = 2na$,

$$\omega_c = \frac{c}{4na}\left[2\pi - \cos^{-1}\left[\frac{1+n^2-6n}{1+n^2+2n}\right]\right]$$

and

$$A = \frac{-cL^2}{2a(1+n)^2}\frac{1}{\sin(4na\omega_c/c)} .$$

The imaginary part of the left-hand side of Eq. (2.7) is singular for $E \to \hbar\omega_c$. Using perturbation theory to estimate the nonsingular parts, we obtain

$$E - E_1' \simeq -i\pi\frac{e^2}{6\pi^2\epsilon_0\hbar m^2}|\mathbf{p}_{10}|^2 E_1'\left[\frac{k_0}{\omega_c}\right]^2 \times \left[\frac{dk}{d\omega_k}\right]_{\hbar\omega_k = E} , \tag{2.8}$$

where

$$E_1' \equiv \frac{e^2}{6\pi^2\epsilon_0\hbar m^2}\sum_{n=0}^{\infty}|\mathbf{p}_{1n}|^2(E_1 - E_n) \times \mathrm{P}[g(E_1 - E_n)]$$

is the standard Lamb shift. To study the band-edge behavior of the isotropic model, we choose $E_1' = \hbar\omega_c$ and substitute the effective-mass expression for ω_k in Eq. (2.8). This gives

$$z^{3/2} \simeq \frac{-i\alpha}{3}\left|\frac{\mathbf{p}_{10}}{m}\right|^2\left[\frac{k_0}{\omega_c}\right]^2\frac{1}{\sqrt{A\omega_c}} , \tag{2.9}$$

for the complex variable $z \equiv (E - \hbar\omega_c)/\hbar\omega_c$, which measures the anomalous part of the Lamb shift and the rate of spontaneous emission. Using the definition $z^{3/2} = |z|e^{3i\theta/2}$ for the complex variable $z = |z|e^{i\theta}$, $0 < \theta < 2\pi$, we find two solutions of Eq. (2.9). The solution at $\theta = \pi$ corresponds to the photon-atom bound state within the photonic band gap, whereas the solution for $\theta = -\pi/3$ (on the second Riemann sheet) lies within the allowed electromagnetic spectrum.

Since the anomalous Lamb shift described by Eq. (2.9) for the case of hydrogen affects the odd-parity $2p_{1/2}$ state and not the even-parity $2S_{1/2}$ state, relative shifts of this nature may be detectable with use of microwaves.[23] Re-

storing correct dimensions to Eq. (2.9), we see that the right-hand side is simply $(\alpha/3)(|\mathbf{p}_{10}|^2/m)/(mc^2)\simeq 10^{-8}$ multiplied by numerical factors of order unity, which may depend on the refractive index n. For the isotropic model described by Eq. (2.1), the splitting of the $2p_{1/2}$ level is larger than the ordinary Lamb shift of the $2S_{1/2}$ level because the exponent of z is $\frac{3}{2}$. This exponent, however, depends sensitively on the dimension d_B of the phase space occupied by band-edge photons of vanishing group velocity. We have overestimated this phase space by assuming that $d\omega_k/dk$ vanishes over the entire sphere $|\mathbf{k}|=\pi/L$. For a real dielectric crystal in three dimensions with an allowed point-group symmetry, the band edge occurs at certain points along the Bragg planes of the lattice. For scalar waves such as electrons, the locus of points for which $|d\omega_k/d\mathbf{k}|=0$ has dimension $d_B=0$. This would be true, for instance, in a many-valley semiconductor crystal for which the bottom of the conduction band occurs at the center of a Bragg plane. The vector nature of the electromagnetic wave modifies this picture, and the phase space near a band edge is enlarged. It was argued previously[7] using a nearly-free-photon approximation for Bragg scattering that the photonic band edge actually lies on a circle of finite radius on the Bragg plane. This suggests that $d_B=1$ in a real photonic crystal as opposed to $d_B=0$ for scalar waves or $d_B=2$ for the isotropic model of Eq. (2.1). In three dimensions, the photonic density of states $\rho(\omega)$ at a band edge ω_c behaves as $(\omega-\omega_c)^{(1-d_B)/2}$ for $\omega\gtrsim\omega_c$. This argument suggests that for a general photonic band structure with band-edge dimension d_B, the exponent of z in Eq. (2.9) becomes $(1+d_B)/2$. For the case $d_B=1$, the left-hand side of Eq. (2.9) is of the form $z/\ln z$, and it follows that the anomalous splitting of the $2p_{1/2}$ level given by $z\equiv(E-\hbar\omega_c)/\hbar\omega_c$ is of order 10^{-7}. This is comparable to the ordinary Lamb shift of the $2S_{1/2}$ level.

A more realistic picture of the band-edge behavior requires the incorporation of Brillouin-zone anisotropy. Consider, for instance, the wave equation for the classical electric field $\mathbf{E}$ in a periodic dielectric,

$$-\nabla^2\mathbf{E}+\nabla(\nabla\cdot\mathbf{E})-\frac{\omega^2}{c^2}\epsilon_{\text{fluct}}(x)\mathbf{E}=\epsilon_0\frac{\omega^2}{c^2}\mathbf{E}\ , \tag{2.10}$$

where the fluctuating part of the dielectric constant describes a fcc lattice of spheres:

$$\epsilon_{\text{fluct}}(x)=\epsilon_1\sum_G U_G e^{i\mathbf{G}\cdot\mathbf{x}}\ , \tag{2.11}$$

where $\{\mathbf{G}\}$ are the reciprocal lattice vectors. The nearly-free-photon approximation follows from treating ϵ_{fluct} as a small perturbation relative to ϵ_0. Setting the dominant Fourier component $U_{\mathbf{G}}=1$, Bragg scattering of photons from wave vector $\mathbf{k}$ to $\mathbf{k}-\mathbf{G}$ leads to the approximate dispersion relations[7]

$$\frac{\omega}{c}=k(\epsilon_0\pm\epsilon_1)^{-1/2} \tag{2.12}$$

and

$$\frac{\omega}{c}=k(\epsilon_0\pm\epsilon_1|1-G^2/2k^2|)^{-1/2}\ , \tag{2.13}$$

corresponding to the polarization vector lying out of the plane (s polarization) and in the plane (p polarization) of Bragg scattering, respectively. For $\epsilon_1/\epsilon_0>\frac{1}{3}$ the phase space for propagation near a band edge is determined by the p-polarization channel. This is a circular photonic valley depicted in Fig. 4. For an anisotropic dispersion relation, the analog of Eq. (2.6a) is

$$\begin{aligned}E-E_1&\simeq\frac{e^2}{4\pi^2\epsilon_0\hbar m^2}\\&\quad\times\sum_{n=0}^{\infty}(E-E_n)\int\frac{|\mathbf{p}_{1n}|^2-|\hat{\mathbf{k}}\cdot\mathbf{p}_{1n}|^2}{\omega_{\mathbf{k}}^2(E/\hbar-\omega_{\mathbf{k}})}d^3\mathbf{k}\\&\simeq\frac{e^2}{4\pi^2\epsilon_0\hbar m^2}|\mathbf{p}_{10}|^2E\int d^3\mathbf{k}\frac{1}{\omega_{\mathbf{k}}^2(E/\hbar-\omega_{\mathbf{k}})}\ .\end{aligned} \tag{2.14}$$

Here we only keep the dominant ($n=0$) term, which becomes singular for $\omega_{\mathbf{k}}$ near conduction-band edge.

Conduction-band states are described by fluctuations (q_1,q_2) away from the circle in Fig. 4. In the effective-mass approximation[7] (model II),

$$\omega=\omega_c+(c^2/2\omega_c)\sum_{i=1}^{3}A_iq_i^2\ , \tag{2.15}$$

with $A_1=(2/\epsilon_1)[(1+\epsilon_1^2)/(1-\epsilon_1^2)]$, $A_2=2(3-1/\epsilon_1)/(1+\epsilon_1)$, $A_3=0$, and $\omega_c^2=(2\epsilon_1G^2c^2)/(1+\epsilon_1)^2$. (We have chosen the unit such that $\epsilon_0=1$.) Setting $E_1=E_c$ and substituting Eq. (2.15) into Eq. (2.14), we obtain

$$z\simeq\frac{e^2}{4\pi^2\epsilon_0\hbar m^2}|\mathbf{p}_{10}|^2\pi\left[\frac{A_2}{2}\right]^{1/2}\left[\frac{G}{\omega_c}\right]^3g_1(z)\ , \tag{2.16}$$

where

$$g_1(z)=\int_{-\infty}^{\infty}du\int_{-\infty}^{\infty}dv\frac{1}{z-(c^2G^2/2\omega_c^2)(A_1u^2+A_2v^2)} \tag{2.17}$$

is a two-dimensional Green's function from which we

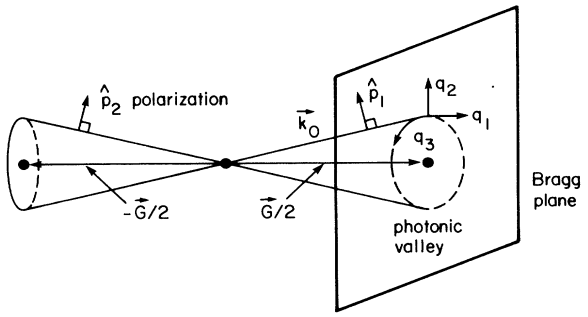

FIG. 4. Creation of a circular photonic valley near the band edge by the Bragg resonance of p-polarized light of wave vector $\mathbf{k}_0+\mathbf{q}$ in a high-dielectric-contrast (ϵ_1/ϵ_0) fcc superlattice. q_1, q_2, and q_3 are the principal axes for photon dispersion.

have $g_1 \sim (\pi/C_1)\ln|z|$, where

$$C_1 = (c^2G^2/2\omega_c^2)(A_1A_2)^{1/2} .$$

In Eq. (2.16) we have integrated over the circumference of the circular photonic valley defined by the coordinate q_3. The remaining integration over $u = q_1/G$ and $v = q_2/G$ are treated in the effective-mass approximation. From Eqs. (2.16) and (2.17), we obtain

$$\frac{z}{\ln|z|} \simeq \frac{\alpha|\mathbf{p}_{10}|^2}{m^2c^2}\frac{\pi\sqrt{A_2/2}}{C_1}\left[\frac{Gc}{\omega_c}\right]^3 \simeq \pi\left[\frac{9(1+\epsilon_1)^3\epsilon_1(1-\epsilon_1)}{2(1+\epsilon_1^2)}\right]^{1/2}\times 10^{-8} . \quad (2.18)$$

From this equation, we obtain $z \simeq (7-8)\times 10^{-7}$ for $\epsilon_1 = 0.4-0.8$. These values are larger than the ordinary Lamb shift.

III. TWO-PHOTON SPONTANEOUS-EMISSION DECAY OF THE PHOTON-ATOM BOUND STATE

Because of the presence of the photonic band gap, single-photon spontaneous emission is inhibited. In this section, we consider spontaneous two-photon emission rate for a hydrogenic $2p$ state. Such an electromagnetic decay mechanism of the photon-bound state may be relevant for the case of an isolated impurity atom in the gap which is not in mechanical contact with the vibrational degrees of freedom of the dielectric host. One example is a dilute atomic vapor which is pumped into void regions of the host material. Although the photon is free to tunnel into the high-dielectric part of the host, we argue in Sec. VI that it is inmune to spontaneous Raman or Brillouin scattering out of the gap. The purely electromagnetic decay mechanism of two-photon emission yields a lifetime for the bound state on the order of days for the $2p_{1/2}$ bound state. This is unlike the two-photon spontaneous emission from the $2s$ state which is $\frac{1}{7}$ sec in vacuum since the $2p_{1/2}$ state must decay by the combination of a dipole and a quadrupole transition rather than a pair of dipole transitions. For simplicity, we assume that the photon dispersion relation is $\omega_k = ck$ and the density of state is that of free photons except near the band gap. Since the dominant contribution to two-photon emission comes from a pair of photons at approximately half the transition frequency, this rate is not significantly altered by the presence of the gap. A reasonable estimate of the lifetime of the bound state follows from assuming free-photon dispersion for all energies. Because of the selection rule, the two-step processes shown in Fig. 5 are allowed. Here one photon is emitted through a dipole (quadrupole) interaction to give an intermediate state and a second emitted through a quadrupole (dipole) interaction to complete the transition to the final state.

The multipolar Hamiltonian can be written as[24]

$$H = H_{\text{atom}} + H_{\text{rad}} + H_{\text{int}} , \quad (3.1)$$

where H_{atom} and H_{rad} are given in Eq. (2.3). The interaction term is defined as

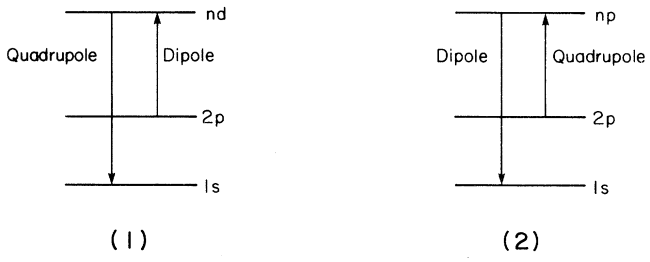

FIG. 5. Two processes allowed in a two-photon transition from the $2p$ to $1s$ state.

$$H_{\text{int}} = -\frac{1}{\epsilon_0}\mu_i d_i^{\perp}(\mathbf{R}) - \frac{1}{\epsilon_0}Q_{ij}\nabla_i d_j^{\perp}(\mathbf{R}) , \quad (3.2)$$

for which

$$\mathbf{d}^{\perp}(\mathbf{R}) = i\sum_{\mathbf{k},\lambda}\left[\frac{\hbar ck\epsilon_0}{2V}\right]^{1/2}[\mathbf{e}^{(\lambda)}(\mathbf{k})a^{(\lambda)}(\mathbf{k})e^{i\mathbf{k}\cdot\mathbf{R}} - \mathbf{e}^{(\lambda)*}(\mathbf{k})a^{\dagger(\lambda)}(\mathbf{k})e^{-i\mathbf{k}\cdot\mathbf{R}}] \quad (3.3)$$

is a transverse field, μ_i is dipole moment, and Q_{ij} is the quadrupole moment given by

$$Q_{ij} = \tfrac{1}{2}r_i r_j . \quad (3.4)$$

Note that since $\nabla\cdot\mathbf{d}^{\perp} = 0$, Q may be taken to be traceless. So Eq. (3.4) can be rewritten as

$$Q_{ij} = \tfrac{1}{2}(r_i r_j - \tfrac{1}{3}r^2\delta_{ij}) . \quad (3.5)$$

The matrix element is calculated using the second-order perturbation

$$M_{fi} = \frac{-i\hbar c}{2\epsilon_0 V}(kk')^{1/2}e_i^{(\lambda)*}(\mathbf{k})e_j^{(\lambda')*}(\mathbf{k}')\beta_{ij}^{om}(k,k') , \quad (3.6)$$

where $\beta_{ij}^{om}(k,k')$ is defined as

$$\beta_{ij}^{om}(k,k') = \sum_r\left[\frac{Q_{il}^{or}k_l\mu_j^{rm}}{E_{ro}-\hbar ck} + \frac{Q_{jl}^{or}k_l'\mu_i^{rm}}{E_{ro}-\hbar ck'} + \frac{\mu_i^{or}Q_{jl}^{rm}k_l'}{E_{ro}-\hbar ck} + \frac{\mu_j^{or}Q_{il}^{rm}k_l}{E_{ro}-\hbar ck'}\right] . \quad (3.7)$$

In this expression, o denotes the $1s$ state and m the $2p$ state. The emitted photons k and k' satisfy energy conservation $E_{mo} = \hbar ck + \hbar ck' = E(2p \rightarrow 1s)$, but are otherwise arbitrary. Here the first two terms in Eq. (3.7) correspond to the process 1 shown in Fig. 5 and the last two terms the process 2. Denote the angular part of dipole and quadrupole moments $\hat{\mu}_k$ and $\hat{Q}_{ij}$, respectively. We have the identity

$$\sum_{l',m'}\langle 1m|\hat{Q}_{ij}|l'm'\rangle\langle l'm'|\hat{\mu}_k|00\rangle = \sum_{l',m'}\langle 1m|\hat{\mu}_k|l'm'\rangle\langle l'm'|\hat{Q}_{ij}|00\rangle . \quad (3.8)$$

From the selection rule, we have $\Delta l=\pm 1$ for dipole transition, $\Delta l=0,\pm 2$ for quadrupole transition. From the definition of Eq. (3.5), we have $\langle 00|\hat{Q}_{ij}|00\rangle=0$. Equation (3.8) becomes

$$\sum_{m'}\langle 1m|\hat{Q}_{ij}|1m'\rangle\langle 1m'|\hat{\mu}_k|00\rangle = \sum_{m''}\langle 1m|\hat{\mu}_k|2m''\rangle\langle 2m''|\hat{Q}_{ij}|00\rangle \ . \quad (3.9)$$

Using Eq. (3.9), Eq. (3.7) can be written as

$$\beta_{ij}^{om}(k,k')=\left[\sum_r \hat{Q}_{il}^{or}\hat{\mu}_j^{rm}\right][A(k,k')k_l+A(k',k)k_l'] \ , \quad (3.10)$$

where

$$\sum_r \hat{Q}_{il}^{or}\hat{\mu}_j^{rm}=\sum_{m'}\langle 00|\hat{Q}_{il}|2m'\rangle\langle 2m'|\hat{\mu}_j|1m\rangle \ , \quad (3.11)$$

$$A(k,k')=\sum_r \frac{Q^{or}\mu^{rm}}{E_{ro}-\hbar ck}+\sum_{r'}\frac{\mu^{or'}Q^{r'm}}{E_{r'o}-\hbar ck'} \ , \quad (3.12)$$

where r and r' represent nd state and np state, respectively. The density of two-photon states at the energy of the emitting state is

$$\rho=\frac{1}{2}\frac{k^2\,dk\,d\Omega}{(2\pi)^3}V\frac{k'^2\,dk'\,d\Omega'}{(2\pi)^3}V\frac{1}{\hbar c\,d\kappa} \ , \quad (3.13)$$

with the constraint $\kappa=k+k'$, where $\hbar c\kappa\equiv E_{mo}$. Here the factor of $\frac{1}{2}$ appears in the above equation to compensate for double counting.

The differential rate by the Fermi rule is, with Eqs. (3.6) and (3.13),

$$d\Gamma=\frac{2\pi}{\hbar}|M_{fi}|^2\rho$$

or

$$d\Gamma=\frac{c}{2^8\pi^5\epsilon_0^2}\sum_{\lambda,\lambda'}e_i^{(\lambda)*}(\mathbf{k})e_j^{(\lambda')*}(\mathbf{k}')e_k^{(\lambda)}(\mathbf{k})e_l^{(\lambda')}(\mathbf{k}')\beta_{ij}^{om}(\mathbf{k},\mathbf{k}')\beta_{kl}^{om*}(\mathbf{k},\mathbf{k}')\frac{k^3k'^3\,dk\,dk'\,d\Omega\,d\Omega'}{d\kappa} \ . \quad (3.14)$$

The sum over polarizations gives

$$\sum_\lambda e_i^{(\lambda)}(\mathbf{k})e_j^{(\lambda)*}(\mathbf{k})=\delta_{ij}-\hat{k}_i\hat{k}_j \ , \quad (3.15)$$

from which we obtain

$$d\Gamma=\frac{c}{2^8\pi^5\epsilon_0^2}(\delta_{ik}-\hat{k}_i\hat{k}_k)(\delta_{jl}-\hat{k}_j'\hat{k}_l')\beta_{ij}^{om}(\mathbf{k},\mathbf{k}')\beta_{kl}^{om*}(\mathbf{k},\mathbf{k}')k^3k'^3\,d\Omega\,d\Omega'\frac{dk\,dk'}{d\kappa} \ . \quad (3.16)$$

The integration over all directions of $\mathbf{k}$ gives the following equations:

$$\begin{aligned}&\int(\delta_{ik}-\hat{k}_i\hat{k}_k)d\Omega=\frac{8\pi}{3}\delta_{ik} \ ,\\ &\int(\delta_{ik}-\hat{k}_i\hat{k}_k)\hat{k}_l\,d\Omega=0 \ ,\\ &\int(\delta_{ik}-\hat{k}_i\hat{k}_k)\hat{k}_l\hat{k}_m\,d\Omega=\frac{16\pi}{15}\delta_{ik}\delta_{lm}-\frac{4\pi}{15}\delta_{im}\delta_{kl}-\frac{4\pi}{15}\delta_{il}\delta_{km} \ .\end{aligned} \quad (3.17)$$

Using these equations, we have

$$\int d\Omega\int d\Omega'(\delta_{ik}-\hat{k}_i\hat{k}_k)(\delta_{jl}-\hat{k}_l'\hat{k}_l')\beta_{ij}^{om}(k,k')\beta_{kl}^{om*}(k,k') = \frac{2^5\pi^2}{15}\left[\sum_{i,j,k}\left|\sum_r \hat{Q}_{ik}^{or}\hat{\mu}_j^{rm}\right|^2\right][k^2A^2(k,k')+k'^2A^2(k',k)] \ . \quad (3.18)$$

In Table I we have tabulated all the nonzero values of $\sum_r \hat{Q}_{ik}^{or}\hat{\mu}_j^{rm}$. Substituting Eq. (3.18) into (3.16) and using Table I, we finally arrive at

$$d\Gamma=\frac{2c}{225\pi}k^3k'^3\frac{dk\,dk'}{d\kappa}[k^2A^2(k,k')+k'^2A^2(k',k)] \ . \quad (3.19)$$

The total two-photon-emission rate Γ is

$$\Gamma=\frac{4c}{225\pi}\int_0^\kappa k^5(\kappa-k)^3A^2(k,\kappa-k)dk \ , \quad (3.20)$$

where we have used the fact that Eq. (3.19) is symmetric about k and k'. Substituting Eq. (3.12) into (3.20) and letting $t=k/\kappa$,

$$\Gamma=\Gamma_0\int_0^1 t^5(1-t)^3\left[\sum_r\frac{Q^{or}\mu^{rm}}{\frac{4}{3}(1\pm 1/r^2)-t}+\sum_{r'}\frac{\mu^{or'}Q^{r'm}}{\frac{4}{3}(1\pm 1/r'^2)-(1-t)}\right]^2 dt \ , \quad (3.21)$$

TABLE I. Nonzero value of the matrix element, where we have defined $\langle 1m|x_i x_j|x_k\rangle \equiv \sum_{m'} \langle 1m|x_i x_j|1m'\rangle\langle 1m'|x_k|00\rangle$.

Matrix element	
$\langle 11\|xy\|x\rangle$	$-i/5\sqrt{6}$
$\langle 11\|xy\|y\rangle$	$1/5\sqrt{6}$
$\langle 11\|xz\|z\rangle$	$1/5\sqrt{6}$
$\langle 11\|yz\|z\rangle$	$-i/5\sqrt{6}$
$\langle 10\|xz\|x\rangle$	$1/5\sqrt{3}$
$\langle 10\|yz\|y\rangle$	$1/5\sqrt{3}$
$\langle 11\|zz\|x\rangle$	$-2/15\sqrt{6}$
$\langle 11\|yy\|x\rangle$	$-2/15\sqrt{6}$
$\langle 11\|xx\|x\rangle$	$4/15\sqrt{6}$
$\langle 11\|xx\|y\rangle$	$2i/15\sqrt{6}$
$\langle 11\|yy\|y\rangle$	$-4i/15\sqrt{6}$
$\langle 11\|zz\|y\rangle$	$2i/15\sqrt{6}$
$\langle 10\|xx\|z\rangle$	$-2/15\sqrt{3}$
$\langle 10\|yy\|z\rangle$	$-2/15\sqrt{3}$
$\langle 10\|zz\|z\rangle$	$4/15\sqrt{3}$

where the minus and plus signs correspond to discrete and continuum states of hydrogen, respectively. Here, $\Gamma_0=(4c/225\pi)\kappa^7\alpha^2 a_0^6=1.968\times10^{-6}s^{-1}$, a_0 is Bohr radius, and α is the fine-structure constant. Note that Γ_0 varies as $(E_{mo})^7$, as compared with $(E_{mo})^3$ for one-photon emission. In order to calculate Eq. (3.21), one must know the moments $\mu(2p\to nd)$, $\mu(np\to 1s)$, $Q(2p\to np)$, and $Q(nd\to 1s)$. We have calculated these quantities for discrete and continuum states.[25] The expressions for discrete n are

$$\mu(2p\to nd)=\frac{2^{10}n^4[(n^3-n)(n^2-4)]^{1/2}(n-1)^{n-4}}{\sqrt{6}(n+2)^{n+4}}, \tag{3.22}$$

$$\mu(np\to 1s)=\frac{2^4 n^3(n^3-n)^{1/2}(n-1)^{n-3}}{(n+1)^{n+3}}, \tag{3.23}$$

$$Q(2p\to np)=-\frac{2^{12}n^5(n^3-n)^{1/2}(n-2)^{n-4}}{\sqrt{6}(n+2)^{n+4}}, \tag{3.24}$$

$$Q(nd\to 1s)=\frac{2^6 n^4[(n^3-n)(n^2-4)]^{1/2}(n-1)^{n-4}}{(n+1)^{n+4}}. \tag{3.25}$$

For continuous n, we have

$$\mu(2p\to nd)=-\frac{2^{10}n^6[(n^2+1)(n^2+4)]^{1/2}}{\sqrt{6}(1-e^{-2\pi n})^{1/2}}\frac{e^{-2n\,\mathrm{arccot}(n/2)}}{(n^2+4)^4}, \tag{3.26}$$

$$\mu(np\to 1s)=\frac{2^4 n^5}{(1-e^{-2\pi n})^{1/2}}\frac{e^{-2n\,\mathrm{arccot}(n)}}{(n^2+1)^{5/2}}, \tag{3.27}$$

$$Q(2p\to np)=\frac{3\times 2^{12}n^7(n^2+1)^{1/2}}{\sqrt{6}(1-e^{-2\pi n})^{1/2}}\frac{e^{-2n\,\mathrm{arccot}(n/2)}}{(n^2+4)^4}, \tag{3.28}$$

$$Q(nd\to 1s)=-\frac{2^6 n^6[(n^2+1)(n^2+4)]^{1/2}}{(n^2+1)^4(1-e^{-2\pi n})^{1/2}}e^{-2n\,\mathrm{arccot}(n)}. \tag{3.29}$$

Using Eqs. (3.21)–(3.29), the integral in Eq. (3.21) is calculated numerically to give $\Gamma=3.773\times10^{-6}\ s^{-1}$ from which we get the lifetime of hydrogen $2p$ state inside the photonic band gap $\tau=1/\Gamma=73.6$ h. Note that for the discrete state two terms in Eq. (3.21) have opposite signs; this interference effect accounts for the large value of τ. This extremely long lifetime, however, will be reduced by the presence of neighboring impurity atoms to which the localized photon can perform either a real or virtual hop. We now proceed to describe elementary cooperative effects when more than one impurity atom is present.

IV. RESONANCE DIPOLE-DIPOLE INTERACTION IN A PERIODIC DIELECTRIC STRUCTURE

Let A and B be identical atoms with nondegenerate ground and excited states $|E_0\rangle$ and $|E_n\rangle$ connected by an electric dipole transition. Assume that, initially, atom A is in its ground state and atom B is in the excited state. Because of spontaneous emission, atom B can emit a photon and make a downward transition to the ground state. Atom A can absorb this photon and go to the excited state. This resonance energy transfer between the pair states $|E_n^A,E_0^B\rangle$ and $|E_0^A,E_n^B\rangle$ is called the resonance dipole-dipole interaction (RDDI). Consider a periodic dielectric structure in which a complete photonic band gap exists. If the transition frequency is inside the band gap, the RDDI must be modified since the RDDI is mediated by the bound photon which cannot propagate through the structure. From the discussion of Sec. II, we see that a photonic bound state exists with a long localization length. The photon can tunnel through the dielectric host and be absorbed resonantly by another atom nearby. In this section we give a detailed analysis of the RDDI. As in Sec. II, we assume that the photon wave function is a transverse plane wave in the allowed continuum and the dispersion relation ω_k is given by Eq. (2.1). The transition frequency $\omega_0\equiv E_{n0}/\hbar$ is inside the band gap. Using the multipolar Hamiltonian in a dipole approximation,

$$H_{\mathrm{int}}=-\frac{1}{\epsilon_0}\boldsymbol{\mu}(A)\cdot\mathbf{d}^{\perp}(\mathbf{R}_A)-\frac{1}{\epsilon_0}\boldsymbol{\mu}(B)\cdot\mathbf{d}^{\perp}(\mathbf{R}_B). \tag{4.1}$$

The matrix element is given by

$$M=\sum_{\mathbf{k},\lambda}\frac{\hbar\omega_k}{2\epsilon_0 V}e_i^{(\lambda)*}(\mathbf{k})e_j^{\lambda}(\mathbf{k})\times\left[\mu_i^{on}(A)\mu_j^{no}(B)\frac{e^{i\mathbf{k}\cdot\mathbf{R}}}{E_{no}-\hbar\omega_k}+\mu_j^{on}(A)\mu_i^{no}(B)\frac{e^{-i\mathbf{k}\cdot\mathbf{R}}}{-E_{no}-\hbar\omega_k}\right], \quad (4.2)$$

where R is the distance between atoms A and B. Using Eq. (3.15) and converting the $\mathbf{k}$ sum to an integral, we obtain

$$M=\frac{1}{2\epsilon_0}\mu_i^{on}(A)\mu_j^{no}(B)\times\int\frac{\hbar\omega_k}{E_{no}^2-\hbar^2\omega_k^2}(\delta_{ij}-\hat{k}_i\hat{k}_j)\times[E_{no}(e^{i\mathbf{k}\cdot\mathbf{R}}-e^{-i\mathbf{k}\cdot\mathbf{R}})+\hbar\omega_k(e^{i\mathbf{k}\cdot\mathbf{R}}+e^{-i\mathbf{k}\cdot\mathbf{R}})]\frac{d^3k}{(2\pi)^3}. \quad (4.3)$$

The first term vanishes because it is an odd function of $\mathbf{k}$. Since the dispersion relation is isotropic, we can integrate over all directions of $\mathbf{k}$ to give

$$M=\frac{1}{2\pi^2\epsilon_0}\mu_i^{on}(A)\mu_j^{no}(B)\int_0^{\infty}\frac{k^2\omega_k^2\tau_{ij}(kR)}{\omega_0^2-\omega_k^2}dk, \quad (4.4)$$

where

$$\tau_{ij}(kR)=(\delta_{ij}-\hat{R}_i\hat{R}_j)\frac{\sin kR}{kR}+(\delta_{ij}-3\hat{R}_i\hat{R}_j)\left[\frac{\cos(kR)}{k^2R^2}-\frac{\sin(kR)}{k^3R^3}\right]. \quad (4.5)$$

For the dispersion relation [Eq. (2.1)], the integrand in Eq. (4.4) has many branch cuts as shown in Fig. 1(b). Unlike the evaluation of RDDI in vacuum, it is not straightforward to apply the residue theorem to evaluate Eq. (4.4). Instead, we calculate Eq. (4.4) numerically as a function of distance R and transition frequency ω_0. Numerical results show that RDDI can be either inhibited or enhanced at short distances $R \ll L$. At longer distances ($R \geq L$), the matrix element oscillates with period of $2L$ and decays exponentially, where L is the lattice constant of the periodic dielectric. A typical RDDI exhibits the asymptotic behavior

$$M\sim\begin{cases}\frac{A}{R^n}\cos\left[\frac{\pi R}{L}+\phi\right]e^{-R/\xi_{\rm loc}}, & R\gg\lambda \quad (4.6a)\\ \frac{A'}{R^{n'}}, & R\ll\lambda, \quad (4.6b)\end{cases}$$

for some amplitudes A, A', exponents n, n', and phase shift ϕ. Here $\xi_{\rm loc}$ is the location length. Generally speaking the amplitude A increases as ω_0 approach to the band edge. Now we discuss the dimer states with $\boldsymbol{\mu}\parallel\mathbf{R}$ (Σ states) and $\boldsymbol{\mu}\perp\mathbf{R}$ (Π states) separately. For Σ states, the relevant projection of τ_{ij} in Eq. (4.5) becomes

$$\tau=-2\left[\frac{\cos(kR)}{k^2R^2}-\frac{\sin(kR)}{k^3R^3}\right]. \quad (4.7)$$

In this case, the exponent n describing the long-distance behavior in Eq. (4.6a) is 2. In Fig. 6(a) we plot M versus distance R for $r=0.1, 0.5$, where we have defined $\omega_0=\omega_{\rm cen}+(r-\frac{1}{2})\Delta\omega$, with $\omega_{\rm cen}$ being the center of the band gap. Here we have chosen the relative gap width $\Delta\omega/\omega_{\rm cen}=5\%$. As we see from Fig. 6(a), RDDI has different behavior in the two regions $R>L$ and $R<L$. For a large distance $R>L$, the phase shift defined

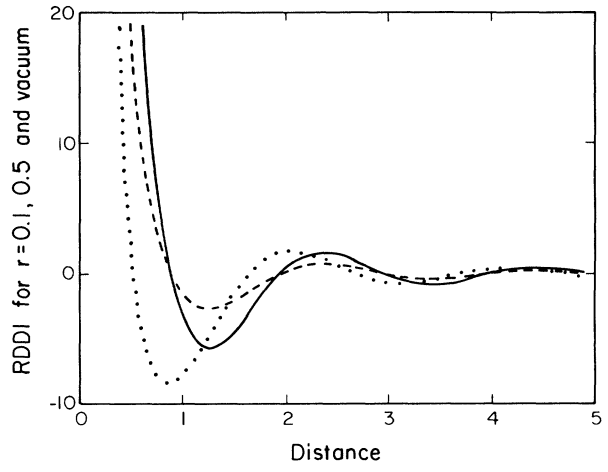

(a)

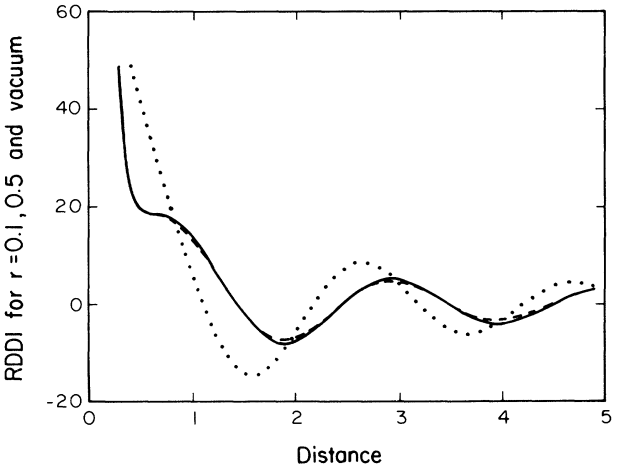

(b)

FIG. 6. RDDI vs R/L for $r=0.1$ (dotted line), 0.5 (dashed line), and vacuum (solid line). Here $\omega_0=\omega_{\rm cen}+(r-\frac{1}{2})\Delta\omega$, where $\omega_{\rm cen}$ is the center of the band gap and $\Delta\omega$ is the bandwidth. (a) For the Σ state we see that the $\pi/2$ phase shift occurs at the center of the band gap. (b) For the Π state the $\pi/2$ phase shift occurs near the band edge.

in Eq. (4.6) changes as we change r. Specifically, at the center of the band gap, the phase shift ϕ is approximately $\pi/2$. As r goes to the band edge, the phase shift goes to zero. For a short distance there is no phase shift ϕ and the exponent $n'=3$ as in the vacuum. For II states, Eq. (4.5) becomes

$$\tau=\frac{\sin(kR)}{kR}+\frac{\cos(kR)}{k^2R^2}-\frac{\sin(kR)}{k^3R^3}\ . \tag{4.8}$$

The exponent n is unity and $n'=3$ in this case. In Fig. 6(b) we plot M versus distance R for $r=0.1,0.5$. Here it is different from Σ states for large distance. The phase shift is zero at the center of the band gap and $\pi/2$ near the band edge. The above calculations have also been done for the relative band gap $\Delta\omega/\omega_{\rm cen}=1\%$ and 10%. The results are similar to that of the 5% relative band gap.

In order to interpret these numerical results, it is instructive to obtain analytic expression for the matrix element M by using an effective-mass approximation to the photon dispersion relation. This is valid for frequencies very close to the photonic band edge and for distance scales $R\gg\lambda$. Consider, for instance, the following dispersion relation:

$$\omega_k^2=\omega_1^2-Ak^2+Bk^4\ , \tag{4.9}$$

with the band edge $\omega_c^2=\omega_1^2-A^2/4B$ at $k_c^2=A/2B$, where A and B are positive constants. Note that ω_k is nonzero at $k=0$. This unphysical aspect can be removed by choosing the contour to bypass this point. Equation (4.4) can be evaluated using the residue theorem by enclosing an upper semicircle on the complex plane. We obtain

$$\begin{aligned}M=&\frac{-1}{2\pi^2\epsilon_0}\mu_i^{on}\mu_j^{no}\frac{\pi\omega_0^2}{2B\rho^4\sin\theta\,R^3}e^{-\xi_{\rm loc}^{-1}R}\\&\times\{(\delta_{ij}-\hat R_i\hat R_j)\rho^2R^2\sin(aR)\\&+(\delta_{ij}-3\hat R_i\hat R_j)[\rho R\cos(aR-\theta/2)\\&-\sin(aR-\theta)]\}\ ,\end{aligned} \tag{4.10}$$

where $\rho^4=k_c^4(\omega_1^2-\omega_0^2)/(\omega_1^2-\omega_c^2)$, $\cos^2\theta=k_c^4/\rho^4$, $\xi_{\rm loc}^{-2}=(k_c^2/2)\{[(\omega_1^2-\omega_0^2)/(\omega_1^2-\omega_c^2)]^{1/2}-1\}$, and $a^2=k_c^2+\xi_{\rm loc}^{-2}$. For the II state, we have

$$\begin{aligned}M=&M_{\rm vac}\frac{\omega_0^2}{\omega_1^2-\omega_0^2}\frac{e^{-\xi_{\rm loc}^{-1}R}}{\sin\theta}\\&\times[\rho^2R^2\sin(aR)+\rho R\cos(aR-\theta/2)\\&-\sin(aR-\theta)]\ ,\end{aligned} \tag{4.11}$$

where $M_{\rm vac}\sim-|\mu|^2/(2\pi^2\epsilon_0R^3)$ is the matrix element of the vacuum when R is small. The condition that Eq. (4.11) has a $\pi/2$ phase shift is $(kR)^3\ll\theta\ll kR$, which can be achieved near the band edge for small R.

The existence of this phase shift has been pointed out by Kurizki[15] who has argued that this can drastically modify the short-distance behavior of RDDI. However, in distance scales $R\ll\lambda$, the effective-mass model is inapplicable. The relevant intermediate photons are no longer restricted to the band edge as revealed by our exact numerical computation. A direct comparison of RDDI in model I with $M_{\rm vac}$ for $R\ll\lambda$ is presented in Fig. 7. It is clear that in all cases the hopping matrix element approaches the vacuum value at short distances.

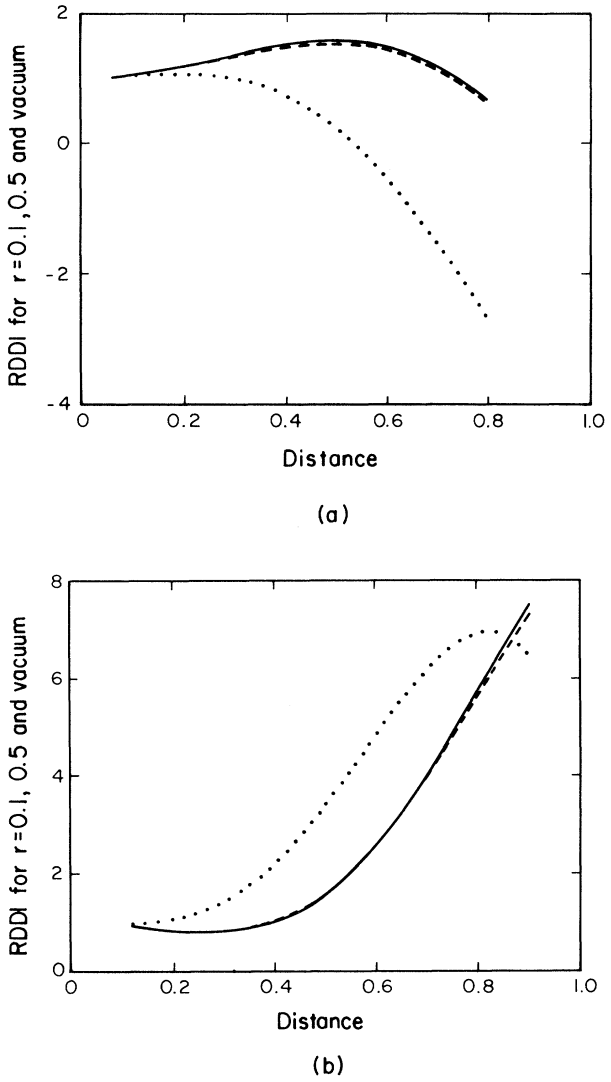

FIG. 7. We plot $(2R^3/\pi)$ times the RDDI for $r=0.1$ (dotted line), 0.5 (dashed line), and vacuum (solid line) at short distance. When $R\to0$, they approach to the same limit. Here we plot $(2R^3/\pi)$, times the RDDI separately for the Σ and II states in (a) and (b), respectively.

V. PHOTON-PHOTON INTERACTION

The strong coupling of photons to the impurity matter field within the photonic band gap gives rise to important photon-photon interactions when more than one electromagnetic excitation is present within the impurity band. In the previous section it was shown that a single excitation can hop from one atom to another by means of a resonance dipole-dipole tunneling process. Likewise,

when two neighboring atoms are excited, the two localized photons can interact by means of the corresponding virtual hop. This virtual hop of a localized photon to another excited atom gives rise to second-harmonic generation and the propagation of the resulting high-energy photon out of the band gap. Assume that atoms A and B are in the excited state with energy E_1 and single-photon spontaneous emission is inhibited. The quantum-electrodynamic interaction leads to a two-atom spontaneous emission where atoms A and B go to ground state and emit a photon with energy $\hbar ck = 2E_1 - 2E_0$. The Hamiltonian is the same as Eq. (4.1). As in the analysis of two-photon spontaneous emission, we assume that the effect of the photonic band gap is simply to eliminate the amplitude for single-photon, single-atom spontaneous emission. For higher-order processes we assume a free-photon dispersion relation $\omega_k = ck$.

There is a simple physical way of understanding the rate of spontaneous second-harmonic generation. Two processes contribute to this emission. As atom A emits a virtual photon through a dipole transition, atom B will absorb this photon and excite to a higher level under a dipole (or a quadrupole) transition and then decay under a quadrupole (or a dipole) transition. Hence the first process corresponds to a dipole-dipole interaction and a quadrupole decay, and the second process to a dipole-quadrupole interaction and a dipole decay. Note that the decay rate for the dipole transition is proportional to $\mu^2\rho$ as compared with $k^2Q^2\rho$ for the quadrupole transition, where ρ is the photon density of states. For the first process the emission rate Γ is proportional to $(\mu^2/R^3)^2(k^2Q^2\rho) \sim (kR)^2(a/R)^8$ and for the second one $\Gamma \sim (\mu Q/R^4)^2(\mu^2\rho) \sim (a/R)^8$. So, at the short distance $kR \ll 1$, the second process is dominant and the emission rate is proportional to $(a/R)^8$.

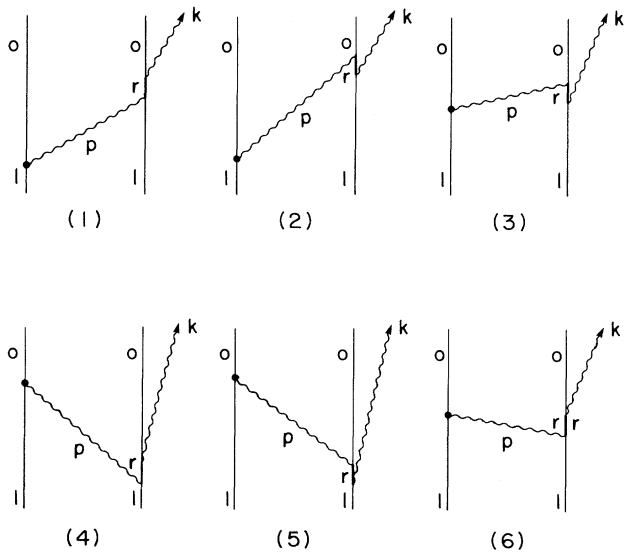

FIG. 8. Time-ordered graphs for two-atom photon-photon interaction resulting in second-harmonic generation.

The leading term, of third order, represents the coupling between the atoms by exchange of virtual photons. Twelve time-ordered graphs contribute to this order, six of which are shown in Fig. 8. The remaining six graphs may be obtained simply by interchanging the identities of atoms A and B. Their contribution to the matrix element are given in Eqs. (5.1)–(5.6):

$$\sum_{\mathbf{p},\lambda,r} A_{jk}(\mathbf{p},\mathbf{k},\lambda)\frac{\mu_j^{r1}(A)Q_{kl}^{or}(A)ik_l + Q_{jl}^{r1}(A)(-ip_l)\mu_k^{or}(A)}{(E_{10}-\hbar cp)(2E_1-E_0-E_r)}\ , \tag{5.1}$$

$$\sum_{\mathbf{p},\lambda,r} A_{jk}(\mathbf{p},\mathbf{k},\lambda)\frac{\mu_k^{r1}(A)Q_{jl}^{or}(A)(-ip_l) + Q_{kl}^{r1}(A)ik_l\mu_j^{or}(A)}{(E_{10}-\hbar cp)(2E_1-E_0-E_r-\hbar cp-\hbar ck)}\ , \tag{5.2}$$

$$\sum_{\mathbf{p},\lambda,r} A_{jk}(\mathbf{p},\mathbf{k},\lambda)\frac{\mu_k^{r1}(A)Q_{jl}^{or}(A)(-ip_l) + Q_{kl}^{r1}(A)ik_l\mu_j^{or}(A)}{(E_{1r}-\hbar ck)(2E_1-E_0-E_r-\hbar cp-\hbar ck)}\ , \tag{5.3}$$

$$\sum_{\mathbf{p},\lambda,r} B_{jk}(\mathbf{p},\mathbf{k},\lambda)\frac{\mu_j^{r1}(A)Q_{kl}^{or}(A)ik_l + Q_{jl}^{r1}(A)ip_l\mu_k^{or}(A)}{(E_{1r}-\hbar cp)(E_{10}-\hbar cp-\hbar ck)}\ , \tag{5.4}$$

$$\sum_{\mathbf{p},\lambda,r} B_{jk}(\mathbf{p},\mathbf{k},\lambda)\frac{\mu_k^{r1}(A)Q_{jl}^{or}(A)ip_l + Q_{kl}^{r1}(A)ik_l\mu_j^{or}(A)}{(E_{1r}-\hbar ck)(E_{10}-\hbar cp-\hbar ck)}\ , \tag{5.5}$$

$$\sum_{\mathbf{p},\lambda,r} B_{jk}(\mathbf{p},\mathbf{k},\lambda)\frac{\mu_j^{r1}(A)Q_{kl}^{or}(A)ik_l + Q_{jl}^{r1}(A)ip_l\mu_k^{or}(A)}{(E_{1r}-\hbar cp)(2E_1-E_0-E_r)}\ , \tag{5.6}$$

where $E_{nm} \equiv E_n - E_m$,

$$A_{jk}(\mathbf{p},\mathbf{k},\lambda) = -i\left[\frac{\hbar ck}{2\epsilon_0 V}\right]^{1/2}\frac{\hbar cp}{2\epsilon_0 V}e^{-i\mathbf{p}\cdot(\mathbf{R}_B-\mathbf{R}_A)}e^{-i\mathbf{k}\cdot\mathbf{R}_A}e_i^{(\lambda)*}(\mathbf{p})e_j^{(\lambda)}(\mathbf{p})e_k^{(\lambda')*}(\mathbf{k})\mu_i^{01}(B)\ , \tag{5.7}$$

and

$$B_{jk}(\mathbf{p},\mathbf{k},\lambda)=-i\left[\frac{\hbar ck}{2\epsilon_0 V}\right]^{1/2}\frac{\hbar cp}{2\epsilon_0 V}e^{i\mathbf{p}\cdot(\mathbf{R}_B-\mathbf{R}_A)}e^{-i\mathbf{k}\cdot\mathbf{R}_A}e_j^{(\lambda)*}(\mathbf{p})e_i^{(\lambda)}(\mathbf{p})e_k^{(\lambda')*}(\mathbf{k})\mu_i^{01}(B)\ . \tag{5.8}$$

Here $(\mathbf{p},\lambda)$ is the wave vector and polarization of the intermediate photon which is exchanged between the atoms, whereas $(\mathbf{k},\lambda')$ describes the state of the final emitted photon.

The matrix element for the graphs shown in Fig. 8 is summed to give

$$\begin{aligned}-i\left[\frac{\hbar ck}{2\epsilon_0 V}\right]^{1/2}&\sum_{\mathbf{p},\lambda,r}\frac{\hbar cp}{2\epsilon_0 V}e_k^{(\lambda')*}(\mathbf{k})\mu_i^{01}e^{-i\mathbf{k}\cdot\mathbf{R}_A}\\&\times\left[\left[\frac{\mu_k^{or}Q_{jl}^{r1}(-ip_l)+Q_{kl}^{or}\mu_j^{r1}ik_l}{E_{0r}+\hbar ck}+\frac{\mu_j^{or}Q_{kl}^{r1}ik_l+Q_{jl}^{or}(-ip_l)\mu_k^{r1}}{E_{1r}-\hbar ck}\right]\frac{e^{-i\mathbf{p}\cdot(\mathbf{R}_B-\mathbf{R}_A)}}{E_{10}-\hbar cp}e_i^{(\lambda)*}(\mathbf{p})e_j^{(\lambda)}(\mathbf{p})\right.\\&\left.+\left[\frac{\mu_k^{or}Q_{jl}^{r1}(ip_l)+Q_{kl}^{or}\mu_j^{r1}ik_l}{E_{or}+\hbar ck}+\frac{\mu_j^{or}Q_{kl}^{r1}ik_l+Q_{jl}^{or}(ip_l)\mu_k^{r1}}{E_{1r}-\hbar ck}\right]\frac{e^{i\mathbf{p}\cdot(\mathbf{R}_B-\mathbf{R}_A)}}{-E_{10}-\hbar cp}e_i^{(\lambda)}(\mathbf{p})e_j^{(\lambda)*}(\mathbf{p})\right]\ .\end{aligned} \tag{5.9}$$

In deriving this equation we have used the energy conservation $2E_1-2E_0=\hbar ck$, from which we have $2E_1-E_0-E_r=E_{or}+\hbar ck$ and $2E_1-E_0-E_r-\hbar cp-\hbar ck=E_{or}-\hbar cp$. Using these two relations, we have combined Eqs. (5.2) and (5.3) to give the second term in the first set of large parentheses, and Eqs. (5.4) and (5.6) the second term in the second set of large parentheses. We have also assumed that atoms A and B are identical.

We obtain the total matrix element for 12 time-ordered graphs:

$$M_3=\left[\frac{\hbar ck}{2\epsilon_0 V}\right]^{1/2}e_k^{(\lambda')*}(\mathbf{k})\mu_i^{01}(e^{-i\mathbf{k}\cdot\mathbf{R}_A}+e^{-i\mathbf{k}\cdot\mathbf{R}_B})\left[V_{ij}(k_{10},R)k_l\beta_{jkl}+\frac{dV_{ij}(k_{10},R)}{dR}\hat{R}_l\beta'_{jkl}\right], \tag{5.10}$$

where

$$\beta_{jkl}=\sum_r\left[\frac{Q_{kl}^{or}\mu_j^{r1}}{E_{0r}+\hbar ck}+\frac{\mu_j^{or}Q_{kl}^{r1}}{E_{1r}-\hbar ck}\right], \tag{5.11a}$$

$$\beta'_{jkl}=\sum_r\left[\frac{Q_{jl}^{r1}\mu_k^{or}}{E_{0r}+\hbar ck}+\frac{\mu_k^{r1}Q_{jl}^{or}}{E_{1r}-\hbar ck}\right], \tag{5.11b}$$

$$V_{ij}(k_{10},R)=\sum_{\mathbf{p},\lambda}\left[\frac{e^{i\mathbf{p}\cdot(\mathbf{R}_A-\mathbf{R}_B)}e_i^{(\lambda)*}(\mathbf{p})e_j^{(\lambda)}(\mathbf{p})}{E_{10}-\hbar cp}+\frac{e^{-i\mathbf{p}\cdot(\mathbf{R}_A-\mathbf{R}_B)}e_i^{(\lambda)}(\mathbf{p})e_j^{(\lambda)*}(\mathbf{p})}{-E_{10}-\hbar cp}\right], \tag{5.12}$$

with $k_{10}=E_{10}/c\hbar$ and $\mathbf{R}=\mathbf{R}_A-\mathbf{R}_B$. Equation (5.12) can be evaluated by the residue theorem to give

$$V_{ij}=\frac{1}{4\pi\epsilon_0 R^3}[(\delta_{ij}-3\hat{R}_i\hat{R}_j)[\cos(k_{10}R)+k_{10}R\sin(k_{10}R)]-(\delta_{ij}-\hat{R}_i\hat{R}_j)k_{10}^2R^2\cos(k_{10}R)]\ . \tag{5.13}$$

So

$$\begin{aligned}\int d\Omega_{\mathbf{k}}\sum_{\lambda'}|M_3|^2=&\frac{\hbar ck}{2\epsilon_0 V}\mu_{i_1}\mu_{i_2}^*\int d\Omega(\delta_{k_1k_2}-\hat{k}_{k_1}\hat{k}_{k_2})[2+2\cos(\mathbf{k}\cdot\mathbf{R})]\\&\times\left[\beta_{j_1k_1l_1}\beta^*_{j_2k_2l_2}V_{i_1j_1}V_{i_2j_2}k^2\hat{k}_{l_1}\hat{k}_{l_2}+2k\hat{k}_{l_1}\hat{R}_{l_2}\beta_{j_1k_1l_1}V_{i_1j_1}\beta'^*_{j_2k_2l_2}\frac{dV_{i_2j_2}}{dR}\right.\\&\left.+\beta'_{j_1k_1l_1}\beta'^*_{j_2k_2l_2}\frac{dV_{i_1j_1}}{dR}\frac{dV_{i_2j_2}}{dR}\hat{R}_{l_1}\hat{R}_{l_2}\right].\end{aligned} \tag{5.14}$$

The angular integral over the directions of propagation of the final photon of wave vector $\mathbf{k}$ in Eq. (5.14) gives

$$\begin{aligned}I_1=&\int d\Omega(\delta_{k_1k_2}-\hat{k}_{k_1}\hat{k}_{k_2})\{[2+2\cos(\mathbf{k}\cdot\mathbf{R})]\}\hat{k}_{l_1}\hat{k}_{l_2}\\=&\frac{4\pi}{15}A-\frac{4\pi}{3}\delta_{l_1l_2}\delta_{k_1k_2}-4\pi(\delta_{l_1l_2}-3\hat{R}_{l_1}\hat{R}_{l_2})\delta_{k_1k_2}\left[\frac{\cos(kR)}{k^2R^2}-\frac{\sin(kR)}{k^3R^3}\right]\\&+4\pi\hat{R}_{l_1}\hat{R}_{l_2}\delta_{k_1k_2}\frac{\sin(kR)}{kR}+4\pi\left[\frac{\sin(kR)}{k^5R^5}-\frac{\cos(kR)}{k^4R^4}\right](3A-15B+105C)\\&+4\pi\frac{\sin(kR)}{k^3R^3}(-A+6B-45C)+4\pi\frac{\cos(kR)}{k^2R^2}(-B+10C)+4\pi\frac{\sin kR}{kR}C\ ,\end{aligned} \tag{5.15a}$$

where

$$A=\delta_{l_1l_2}\delta_{k_1k_2}+\delta_{l_1k_1}\delta_{l_2k_2}+\delta_{l_1k_2}\delta_{l_2k_1}\ , \tag{5.15b}$$

$$B=\delta_{l_1l_2}\hat{R}_{k_1}\hat{R}_{k_2}+\delta_{l_1k_1}\hat{R}_{l_2}\hat{R}_{k_2}+\delta_{l_1k_2}\hat{R}_{l_2}\hat{R}_{k_1}+\delta_{l_2k_1}\hat{R}_{l_1}\hat{R}_{k_2}+\delta_{l_2k_2}\hat{R}_{l_1}\hat{R}_{k_1}+\delta_{k_1k_2}\hat{R}_{l_1}\hat{R}_{l_2}\ , \tag{5.15c}$$

$$C=\hat{R}_{l_1}\hat{R}_{l_2}\hat{R}_{k_1}\hat{R}_{k_2}\ , \tag{5.15d}$$

$$\begin{aligned}I_2&=2\int d\Omega(\delta_{k_1k_2}-\hat{k}_{k_1}\hat{k}_{k_2})[2+2\cos(\mathbf{k}\cdot\mathbf{R})]k_{l_1}\\&=32\pi\left[\left[\frac{\cos(kR)}{k^3R^3}-\frac{\sin(kR)}{k^4R^4}\right][-3(\delta_{l_1k_2}\hat{R}_{k_1}+\delta_{l_1k_1}\hat{R}_{k_2}+\delta_{k_1k_2}\hat{R}_{l_1})+15\hat{R}_{k_1}\hat{R}_{k_2}\hat{R}_{l_1}]\right.\\&\quad\left.-\frac{\sin(kR)}{k^2R^2}[(\delta_{l_1k_2}\hat{R}_{k_1}+\delta_{l_1k_1}\hat{R}_{k_2}+\delta_{k_1k_2}\hat{R}_{l_1})-6\hat{R}_{k_1}\hat{R}_{k_2}\hat{R}_{l_1}]-\frac{\cos(kR)}{kR}\hat{R}_{k_1}\hat{R}_{k_2}\hat{R}_{l_1}\right]\ .\end{aligned} \tag{5.16}$$

Now we examine the small-distance behavior, i.e., $kR\ll1$. Under this condition the third term in Eq. (5.14) is dominant, and so we have

$$\int d\Omega\sum_{\lambda'}|M_3|^2\simeq\frac{\hbar ck}{2\epsilon_0V}\frac{32\pi}{3}\left[\frac{3}{4\pi\epsilon_0R^4}\right]^2\frac{\hbar c\alpha^3a^8}{k^2}\beta'^2\ , \tag{5.17}$$

where we have used Eq. (5.13). Here a is the Bohr radius, α is the fine-structure constant, and β' is a dimensionless quantity:

$$\beta'=\sum_r\left[\frac{Q^{r1}\mu^{or}}{k_{or}/k+1}+\frac{\mu^{r1}Q^{or}}{k_{1r}/k-1}\right]\ , \tag{5.18}$$

where μ and Q are dimensionless given by Eqs. (3.22)–(3.29). The two-atom spontaneous emission rate Γ is

$$\Gamma=\frac{2\pi}{\hbar}\int d\Omega\sum_{\lambda'}|M_3|^2\rho\ , \tag{5.19}$$

where ρ is the density of states given by

$$\rho=\frac{k^2V}{(2\pi)^3\hbar c}\ . \tag{5.20}$$

Substituting Eqs. (5.17) and (5.20) into Eq. (5.19), we obtain, for $kR\ll1$,

$$\Gamma=48\alpha^3/kc\left[\frac{a}{R}\right]^8\beta'^2\ . \tag{5.21}$$

The numerical calculation gives $\beta'^2\simeq0.31$. We finally obtain the transition rate Γ when $kR\ll1$:

$$\Gamma\simeq9\times10^{10}\left[\frac{a}{R}\right]^8/\text{sec}\ . \tag{5.22}$$

For instance, if we assume the distance between two atoms is 5 Å from Eq. (5.22), we get $\Gamma=1.4\times10^3$/sec. Note that we only considered the short-distance behavior so the factor of $e^{-\xi_{\rm loc}^{-1}R}$ has been omitted.

VI. VIBRATIONAL RELAXATION MECHANISMS

So far we have considered only electromagnetic relaxation processes for the decay of the photon-atom bound state. For an atom placed within the solid part of the dielectric host material, this picture may be considerably modified by the interaction of the vibrational modes of the host with the impurity atom. We first consider the effect of Raman scattering and Brillouin scattering. During the scattering, part of the photon energy is absorbed by the optical phonon or acoustic phonon such that the scattered photon is out of the photonic band gap. The interaction Hamiltonian can be written as

$$H_1=\sum_{l,l',k}\kappa_{l,l',k}b_k(a_l^\dagger-a_l)(a_{l'}^\dagger-a_{l'})+\text{c.c.}\ , \tag{6.1}$$

where a_l and b_k are the annihilation operators for photon and phonon, respectively. The coupling constant $\kappa_{l,l',k}$ can be written as[26]

$$\kappa_{l,l',k}=\frac{-i\gamma}{4\epsilon}\left[\frac{\hbar^3}{2VB}\right]^{1/2}(\omega_l\omega_{l'}\omega_k)^{1/2}\times\int_V e^{ikx}\mathbf{E}_l(\mathbf{r})\cdot\mathbf{E}_{l'}(\mathbf{r})dV\ , \tag{6.2}$$

where $\mathbf{E}$ is the electric field associated with the photon, γ is the electrostrictive coefficient, and B is the bulk modulus. Here ω_l and ω_k are frequencies for photon and phonon, respectively. In the standard case of propagating photons, the overlap integral of the incident and scattered fields appearing in Eq. (6.2) is finite since both $\mathbf{E}_l$ and $\mathbf{E}_{l'}$ are proportional to $1/\sqrt{V}$, where V is the volume of the sample and the integration volume is also V. In our case the incident wave is a localized photon and the resulting integration volume is finite $\sim\xi_{\rm loc}^3$. The scattered wave is extended, however, and the overlap integral now scales as $1/\sqrt{V}$. So the transition rate $\Gamma=(2\pi/\hbar)\rho|M|^2$ is proportional to $1/V$, which goes to zero in the thermodynamic limit.

In conclusion, there is no decay of the bound state by spontaneous Raman or Brillouin scattering out of the photonic band gap. Such a direct photon-phonon process is forbidden because of the vanishing overlap between the initial localized and final extended states.

An alternative relaxation process arises through the influence of phonons on the electronic degrees of freedom of the excited atom. The electromagnetic field drives charge-density oscillations within the impurity atom, which in turn can drive vibrational degrees of freedom via the electron-phonon coupling. If the energy of the absorbed or emitted phonon is sufficient to couple the localized photon to extended states outside of the photonic band gap, the bound state will decay via the appropriate phonon sideband. To illustrate the nonlinear interaction of the electron-phonon system, let us examine a two-oscillator model whose Hamiltonian is given by

$$H=\tfrac{1}{2}\dot{x}^2+\tfrac{1}{2}\dot{y}^2+\tfrac{1}{2}\omega_1^2x^2+\tfrac{1}{2}\omega_2^2y^2+\tfrac{1}{2}\gamma\omega_1^2x^2y \ . \tag{6.3}$$

Here x represents the electron coordinate and y represents a phonon coordinate. The equations of motion can be written as

$$\ddot{x}+\omega_1^2x+\gamma\omega_1^2xy=0 \ , \tag{6.4}$$

$$\ddot{y}+\omega_2^2y+\tfrac{1}{2}\gamma\omega_1^2x^2=0 \ . \tag{6.5}$$

If we substitute the zeroth-order solution $x=X\exp(\pm i\omega_1 t)$ and $y=Y\exp(\pm i\omega_2 t)$ into the above equations, we obtain, by successive approximation, a series of components with frequencies $|\omega_1+n\omega_2|$ for x oscillation. Under oscillating external electromagnetic force $F\exp(-i\omega t)$ acting upon Eq. (6.4), the resonance absorption takes place not only at $\omega=\omega_1$, but also at $|\omega_1+n\omega_2|$: The external force directly excites a quantum $\hbar\omega_1$ of the x oscillator, which in turn causes, through the nonlinear interaction, multiple production of quanta $\hbar\omega_2$ of the y oscillator. This part of the absorption spectra corresponding to simultaneous excitation of another oscillator not directly subject to the external force is referred to as a sideband.[27]

A quantitative theory of vibrational relaxation requires an accurate estimate of the relevant electron-phonon coupling on distance scales much shorter than the interatomic spacing of the dielectric host. This will depend crucially on the nature of the impurity atom and its local environment. This will vary considerably from a material to another, and our aim here is to simply present a qualitative discussion which may provide some guide to the choice of materials in an actual experiment.

Let $H_L=K_L(p)+U_L(q)$ be the Hamiltonian for the lattice vibrations of the crystal and $\mathcal{H}_e(\mathbf{p},\mathbf{r};q)$ be the atomic Hamiltonian for the localized electron in the presence of phonons. Here $\mathbf{r}$ and $\mathbf{p}$ denote, respectively, the coordinate and momentum of the electron, while multidimensional $q\equiv(q_1,q_2,\ldots)$ and $p\equiv(p_1,p_2,\ldots)$ denote those of the lattice vibrations. The total Hamiltonian of the electron-phonon system is given by $H_{\rm tot}=\mathcal{H}_e+H_L$. Using the adiabatic approximation, one solves the Schrödinger equations for the electron and lattice vibration, respectively:

$$\mathcal{H}_e(\mathbf{p},\mathbf{r};q)\Phi_\lambda(\mathbf{r};q)=\varepsilon_\lambda(q)\Phi_\lambda(\mathbf{r};q) \ , \tag{6.6}$$

$$H_\lambda\equiv[K_L(p)+W_\lambda(q)]\chi_{\lambda n}(q)=E_{\lambda n}\chi_{\lambda n}(q) \ , \tag{6.7}$$

where $W_\lambda(q)\equiv\varepsilon_\lambda(q)+U_L(q)$ is the adiabatic potential and n denotes for the vibrational state. The energy and wave function of the electron-phonon system are given by $E_{\lambda n}$ and $\Psi_{\lambda n}(\mathbf{r},q)=\Phi_\lambda(\mathbf{r};q)\cdot\chi_{\lambda n}(q)$, respectively. In order to calculate the line shape, we introduce the generating function $f(t)$, which is the autocorrelation function of the atomic dipole moment operator:

$$f(t)\equiv\int_{-\infty}^{+\infty}dE\,F(E)\exp(-iEt/\hbar) \ , \tag{6.8}$$

where $F(E)$ is the optical absorption spectrum corresponding to the electronic transition $\lambda\rightarrow\lambda'$ given by

$$F(E)=\sum_{n,n'}w_{\lambda n}|P_{\lambda n,\lambda' n'}|^2\delta(E-E_{\lambda' n'}+E_{\lambda n}) \ . \tag{6.9}$$

Here P is the electric dipole moment and $w_{\lambda n}\propto\exp(-\beta E_{\lambda n})$. Inserting Eq. (6.9) into Eq. (6.8) and making use of the density matrix $\rho_\lambda(\beta)=\exp(-\beta H_\lambda)$, with H_λ defined in Eq. (6.7), we can rewrite Eq. (6.8) in terms of the trace operation tr_L over the lattice system alone:

$$f(t)=\mathrm{tr}_L\{\rho_\lambda(\beta)[\exp(i\hbar^{-1}H_\lambda t)P_{\lambda\lambda'}\times\exp(-i\hbar^{-1}H_{\lambda'}t)]P_{\lambda'\lambda}\}/\mathrm{tr}_L[\rho_\lambda(\beta)] \ . \tag{6.10}$$

To calculate $f(t)$, we expand $\mathcal{H}_e$ around $q=0$ and keep only the linear term:

$$\mathcal{H}_e=H_e(\mathbf{p},\mathbf{r})+H'(\mathbf{r},q) \ , \tag{6.11}$$

$$H'=-\sum_j(2\omega_j/\hbar)^{1/2}\gamma_j(\mathbf{r})q_j=-\sum_{j,\lambda,\lambda'}\gamma_{j\lambda\lambda'}a_\lambda^\dagger a_{\lambda'}(b_j+b_j^\dagger) \ , \tag{6.12}$$

where ω_j is the normal-mode frequency, and b_j and a_λ are annihilation operators for phonon and electron, respectively. Here $\gamma_j(\mathbf{r})=-(\hbar/2\omega_j)^{1/2}(\partial\mathcal{H}_e/\partial q_j)|_{q=0}$ and $\gamma_{j\lambda\lambda'}\equiv\int d\mathbf{r}\,\phi_\lambda^*(\mathbf{r})\gamma_j(\mathbf{r})\phi_{\lambda'}(\mathbf{r})$, where ϕ_λ is the electronic eigenstate. Note that Eq. (6.12) is of the x^2y form in Eq. (6.3) and in our case describes the emission or absorption of phonons when there is a change in the electronic state. For this order of electron-phonon interaction, an approximate evaluation of Eq. (6.10) has been given by Nakajima, Toyozawa, and Abe,[27] who show that

$$f(t)=|P_{\lambda'\lambda}|^2\exp[-i\hbar^{-1}E_0t-S+S_+(t)+S_-(t)] \ , \tag{6.13}$$

where

$$S_+=\sum_j\frac{\gamma_j^2}{\hbar^2\omega_j^2}(N_j+1)e^{i\omega_j t} \ , \tag{6.14}$$

$$S_-=\sum_j\frac{\gamma_j^2}{\hbar^2\omega_j^2}N_je^{-i\omega_j t} \ , \tag{6.15}$$

$$S=S_+(0)+S_-(0) \ , \tag{6.16}$$

where E_0 is the thermal-excitation energy and $N_j=(e^{\beta\omega_j}-1)^{-1}$ is the average number of phonons per mode in thermal equilibrium.

Expanding $f(t)$ in terms of $S_{\pm}(t)$, it is not hard to see that the term $[S_+(t)]^n[S_-(t)]^{n'}$ corresponds to the phonon sideband consisting of the spectral lines at $E=E_0+\sum^{n'}\hbar\omega_j-\sum^{n}\hbar\omega_j$ with intensity $\exp(-S)$ for the zero-phonon line, $S\exp(-S)$ for the one-phonon sideband, etc. A simple model for the lifetime follows from the assumption that $S_+=S_+(0)e^{i\omega_0 t-\Gamma_0 t}$. Suppose, for instance, that the system is at zero temperature so that the phonon absorption term $S_-(t)=0$ and $S_+(0)=S$. The rate of decay of an n-phonon-emission process at photon energy $E_0-n\hbar\omega_0$ is given by $n\Gamma_0$. The probability of decay via this channel is given by $p_n=(S^n/n!)e^{-S}$. Hence the total rate of decay Γ of the photon-atom bound state by multiple-phonon-emission processes is given by

$$\Gamma=\Gamma_0\sum_{n=1}^{\infty}np_n=S\Gamma_0\ . \tag{6.17}$$

In the limit $S\ll 1$ required for the validity of this perturbative analysis, it is apparent that the leading contribution to the total rate of decay Γ comes from the single-phonon emission rate $Se^{-S}\Gamma_0$. In a dielectric material with a photonic band gap $\Delta\omega/\omega_0\simeq 5\%$ and for an atomic transition of ~ 2 eV placed at the center of this gap, the phonon required to couple the localized photon out of the gap must have an energy of at least 0.5 eV. In the absence of such a high-energy phonon, the total rate of decay must accordingly be modified to become $\Gamma=S(1-e^{-S})\Gamma_0\simeq S^2\Gamma_0$ for two-phonon emission, etc. It is likely that for the size of photonic band gap currently available one or two optical phonons of the dielectric will be sufficient to cause a decay of the photon-atom bound state. The coefficients $S_{\pm}(0)$ are determined by the coupling strength γ_j, which in wave-vector space takes the form

$$\gamma_k=V_k\,\Delta\rho_k(m,n)\ , \tag{6.18}$$

where $\Delta\rho_k(m,n)\equiv\int d^3r\,e^{i\mathbf{k}\cdot\mathbf{r}}[|\phi_m(\mathbf{r})|^2-|\phi_n(\mathbf{r})|^2]$ describes the change in electronic charge density associated with the desired atomic transition. The standard continuum (long-wavelength) forms of the electron-phonon coupling are

$$V_k=\frac{ie}{k}\left[\frac{2\pi\hbar\omega_k}{V}\left[\frac{1}{\epsilon_\infty}-\frac{1}{\epsilon_0}\right]\right]^{1/2}, \tag{6.19}$$

for longitudinal-optical phonons in a polar solid and

$$V_k=-i\left[\frac{\hbar E_d^2}{2NMc_s}\right]^{1/2}k^{1/2}\ , \tag{6.20}$$

for acoustic phonons. Here ϵ is the dielectric constant, E_d is the deformation potential, and c_s is the speed of sound. Since V_k may require considerable alteration on short (~ 0.5 Å) length scales, we leave V_k as parameter to be determined experimentally. For optical phonons at zero temperature,

$$S_+(t)=\sum_{\mathbf{k}}\frac{\gamma_{\mathbf{k}}^2}{\hbar^2\omega_{\mathbf{k}}^2}e^{i\omega_{\mathbf{k}}t}=\int_0^{\infty}N(\omega)d\omega\frac{\gamma_{k(\omega)}^2}{\hbar^2\omega^2}e^{i\omega t}\ . \tag{6.21}$$

Here $N(\omega)$ is the density of states for optical phonon. To obtain a qualitative picture, we assume that the optical spectrum is characterized by a center frequency ω_0 and some narrow width Γ_0. This can be implemented by a Lorentzian model density of states $N(\omega)=(3N/\pi)\Gamma_0/[(\omega-\omega_0)^2+\Gamma_0^2]$. Then Eq. (6.21) can be written as

$$\begin{aligned}S_+(t)&=\frac{3N}{\pi}\int_0^{\infty}d\omega\frac{\Gamma_0}{(\omega-\omega_0)^2+\Gamma_0^2}\frac{\gamma_{k(\omega)}^2}{\hbar^2\omega^2}e^{i\omega t}\\&\simeq 3N\frac{\gamma_{k(\omega_0)}^2}{\hbar^2\omega_0^2}e^{i\omega_0 t-\Gamma_0 t}\ .\end{aligned} \tag{6.22}$$

This is precisely of the form anticipated in our model describing the lifetime. It is interesting to note that the total decay rate $S_+(0)\Gamma_0$ is governed not only by the electron-phonon coupling strength, but also by the width of the optical-phonon band. For phonons with no dispersion ($d\omega_k/dk=0$), the excited atom does not decay, but will exhibit the analog of Jaynes-Cummings[28] oscillations. Also, the factor $(\Delta\rho_k)^2$ suggests that a considerable enhancement of the lifetime will be possible if the relevant electronic transition is of an intrashell rather than an intershell transition. The intershell $2p\rightarrow 1s$ transition example used in discussing electromagnetic decay mechanisms in fact involves a relatively large electronic charge redistribution.

VII. SUMMARY AND CONCLUSIONS

In summary, we have shown, using a simple model of photonic band structure, that atomic and molecular spectroscopy in a dielectric with a photonic band gap is qualitatively modified from its nature in vacuum. For an isolated atom with a transition frequency in the band gap of the dielectric, single-photon spontaneous emission is inhibited and a quantum-electrodynamic bound state of the photon to the atom is formed. Near a band edge, the dressing of the atom by photons with a finite effective mass becomes strong enough to split the atomic level by an observable amount. This splitting occurs in the absence of any external radiation field. The occurrence of these phenomena suggests that suitably prepared dielectric microstructures present a fundamentally new arena for the study of radiation-matter interactions. For the case of a $2p\rightarrow 1s$ atomic transition, the photon-atom bound state has a high degree of electromagnetic stability because of the atomic selection rules governing the next-higher-order decay mechanism. Two-photon spontaneous emission involves the combination of a dipole and a quadrupole transition, leading to a lifetime on the scale of days. When there is a collection of identical impurity atoms with spacing $R\ll\lambda$, the transition wavelength, novel cooperative effects arise. Electromagnetic coupling of neighboring atoms takes place by means of a modified resonance dipole-dipole interaction since the bound photon can tunnel many wavelengths within its localization length. This tunneling process leads to the formation of a photonic impurity band within the photonic band gap in analogy with impurity bands in semiconductors. When

many atoms in the impurity band are excited, nonlinear photon-photon interactions mediated by the resonant coupling of light to the atoms arise. The strength of this nonlinear interaction may be controlled by varying the interatomic spacing R. This nonlinear photonic impurity band defines a novel quantum many-body system which may exhibit macroscopic coherence in the form of superradiance and laser activity. A more detailed understanding of nonelectromagnetic dissipative mechanisms is required to answer this question. For a localized photon, spontaneous Raman or Brillouin scattering into an extended state is forbidden. However, decay of the photon-atom bound state may occur by direct electron-phonon coupling within the dielectric host. In this case photon emission is accompanied by one or more phonon sidebands. We have calculated the two-atom photon-photon interaction and the two-atom spontaneous decay rate is proportional to $(a/R)^8$ at short distance. The analysis we have presented was based on the preparation of a periodic dielectric exhibiting a complete photonic band gap. We anticipate, however, that similar physics will emerge in disordered dielectrics for which there is a pseudogap in the photon density of states containing localized electromagnetic modes.

ACKNOWLEDGMENTS

This work was supported in part by the Natural Sciences and Engineering Research Council of Canada and the Ontario Laser and Lightwave Centre.

APPENDIX

In this appendix we will derive Eq. (2.1). We first consider the following Schrödinger equation at one dimension:

$$-\frac{\hbar^2}{2m}\nabla^2\Psi(x)+V(x)\Psi=E\Psi\ , \tag{A1}$$

where

$$V(x)=\sum_{m=-\infty}^{\infty}u(x-mL) \tag{A2}$$

and

$$u(x)=\begin{cases}-V_0, & |x|<a\\ 0, & \text{otherwise}\ .\end{cases} \tag{A3}$$

From Ref. 29 we obtain the dispersion relation as

$$\cos(kL)=\frac{t^2-r^2}{2t}e^{-i\kappa L}+\frac{1}{2t}e^{i\kappa L}\ , \tag{A4}$$

where $\kappa=(2mE/\hbar^2)^{1/2}$. Here t and r are, respectively, the transmission and reflection coefficients for a single potential well:

$$V(x)=\begin{cases}-V_0, & |x|<a\\ 0, & \text{otherwise}\ .\end{cases} \tag{A5}$$

The coefficients t and r can be defined through wave function Ψ as

$$\Psi(x)=\begin{cases}e^{i\kappa x}+re^{-i\kappa x}, & x<-a\\ te^{i\kappa x}, & x>a\ .\end{cases} \tag{A6}$$

Using the scattering matrix,[30] we have

$$\begin{bmatrix}r\\1\end{bmatrix}=\begin{bmatrix}\left[\cos(2\kappa' a)-i\frac{\epsilon'}{2}\sin(2\kappa' a)\right]e^{2i\kappa a} & i\frac{\eta'}{2}\sin(2\kappa' a)\\ -i\frac{\eta'}{2}\sin(2\kappa' a) & \left[\cos(2\kappa' a)+i\frac{\epsilon'}{2}\sin(2\kappa' a)\right]e^{-2i\kappa}\end{bmatrix}\begin{bmatrix}0\\t\end{bmatrix}\ , \tag{A7}$$

where $\epsilon'\equiv\kappa'/\kappa+\kappa/\kappa'$, $\eta'\equiv\kappa/\kappa'-\kappa'/\kappa$, and $\kappa'\equiv[2m(E+V_0)/\hbar^2]^{1/2}$. From Eq. (A7) it follows that

$$\begin{aligned}\frac{t^2-r^2}{2t}&=e^{2i\kappa a}\frac{1+\frac{n'^2}{4}\sin^2(2\kappa' a)}{2\cos(2\kappa' a)+i\epsilon\sin(2\kappa' a)}\\ &=e^{2i\kappa a}[2\cos(2\kappa' a)-i\epsilon\sin(2\kappa' a)]\end{aligned} \tag{A8}$$

and

$$\frac{1}{2t}=\left[\frac{t^2-r^2}{2t}\right]^*\ . \tag{A9}$$

From Eqs. (A4), (A8), and (A9), we obtain

$$\cos(kL)=\cos(2\kappa a-\kappa L)\cos(2\kappa' a)+\frac{\epsilon'}{2}\sin(2\kappa a-\kappa L)\sin(2\kappa' a)\ . \tag{A10}$$

In our case $\kappa=\omega/c$, $\kappa'=n\omega/c$, and $\epsilon'=n+1/n$. Finally, we obtain

$$\cos(kL)=\cos[(2a-L)\omega]\cos(2n\omega a)+\frac{1+n^2}{2n}\sin[(2a-L)\omega]\sin(2n\omega a)\ , \tag{A11}$$

which is the same as Eq. (2.1) if we denote $b=L-2a$.

[1]A. Z. Genack, Phys. Rev. Lett. **58**, 2043 (1987).
[2]J. M. Drake and A. Z. Genack, Phys. Rev. Lett. **63**, 259 (1989).
[3]E. Yablonovitch and T. Gmitter, Phys. Rev. Lett. **63**, 1950 (1989).
[4]A. Z. Genack and N. Garcia (unpublished).
[5]S. John, Phys. Rev. Lett. **53**, 2169 (1984).
[6]P. W. Anderson, Philos. Mag. B **52**, 505 (1985).
[7]S. John, Phys. Rev. Lett. **58**, 2486 (1987).
[8]P. W. Anderson, Phys. Rev. **109**, 1492 (1958).
[9]M. van Albada and A. Lagendijk, Phys. Rev. Lett. **55**, 2692 (1985).
[10]P. E. Wolf and G. Maret, Phys. Rev. Lett. **55**, 2695 (1985).
[11]S. Etemad, R. Thompson, and M. J. Andrejco, Phys. Rev. Lett. **57**, 575 (1986). M. Kaveh, M. Rosenbluh, I. Edrei, and I. Freund, *ibid.* **57**, 2049 (1986).
[12]K. M. Ho, C. T. Chan, and C. M. Soukoulis, Phys. Rev. Lett. **65**, 3152 (1990); Z. Zhang and S. Satpathy, *ibid.* **65**, 2650 (1990); E. Yablonovitch, T. J. Gmitter, and K. M. Leung (unpublished).
[13]S. John and J. Wang, Phys. Rev. Lett. **64**, 2418 (1990).
[14]B. R. Mollow, Phys. Rev. **188**, 1969 (1969).
[15]G. Kurizki, Phys. Rev. A **42**, 2915 (1990).
[16]S. John and R. Rangarajan, Phys. Rev. B **38**, 10101 (1988).
[17]E. N. Economou and A. Zdetsis, Phys. Rev. B **40**, 1334 (1989).
[18]S. Satpathy, Z. Zhang, and M. R. Salehpour, Phys. Rev. Lett. **64**, 1239 (1990).
[19]K. M. Leung and Y. F. Liu, Phys. Rev. Lett. **65**, 2646 (1990).
[20]H. A. Bethe, Phys. Rev. Lett. **72**, 339 (1947).
[21]See, for instance, J. Bjorken and S. Drell, *Relativistic Quantum Mechanics* (McGraw-Hill, New York, 1964), pp. 35–42.
[22]H. A. Bethe, L. M. Brown, and J. R. Stehn, Phys. Rev. **77**, 370 (1950).
[23]W. E. Lamb and R. C. Retherford, Phys. Rev. **72**, 241 (1947).
[24]D. P. Craig and T. Thirunamachandran, *Molecular Quantum Electrodynamic* (Academic, New York, 1984).
[25]H. A. Bethe and E. E. Salpeter, *Quantum Mechanics of One and Two Electron Atoms* (Springer-Verlag, Berlin, 1957).
[26]A. Yariv, IEEE J. Quantum Electron. **QE-1**, 28 (1965).
[27]S. Nakajima, Y. Toyozawa, and R. Abe, *The Physics of Elementary Excitations* (Springer-Verlag, Berlin, 1980).
[28]E. T. Jaynes and F. W. Cummings, Proc. IEEE **51**, 89 (1963).
[29]N. W. Ashcroft and N. D. Mermin, *Solid State Physics* (Saunders College, Philadelphia, 1976), pp. 146–147.
[30]E. Merzbacher, *Quantum Mechanics* (Wiley, New York, 1970), p. 108.